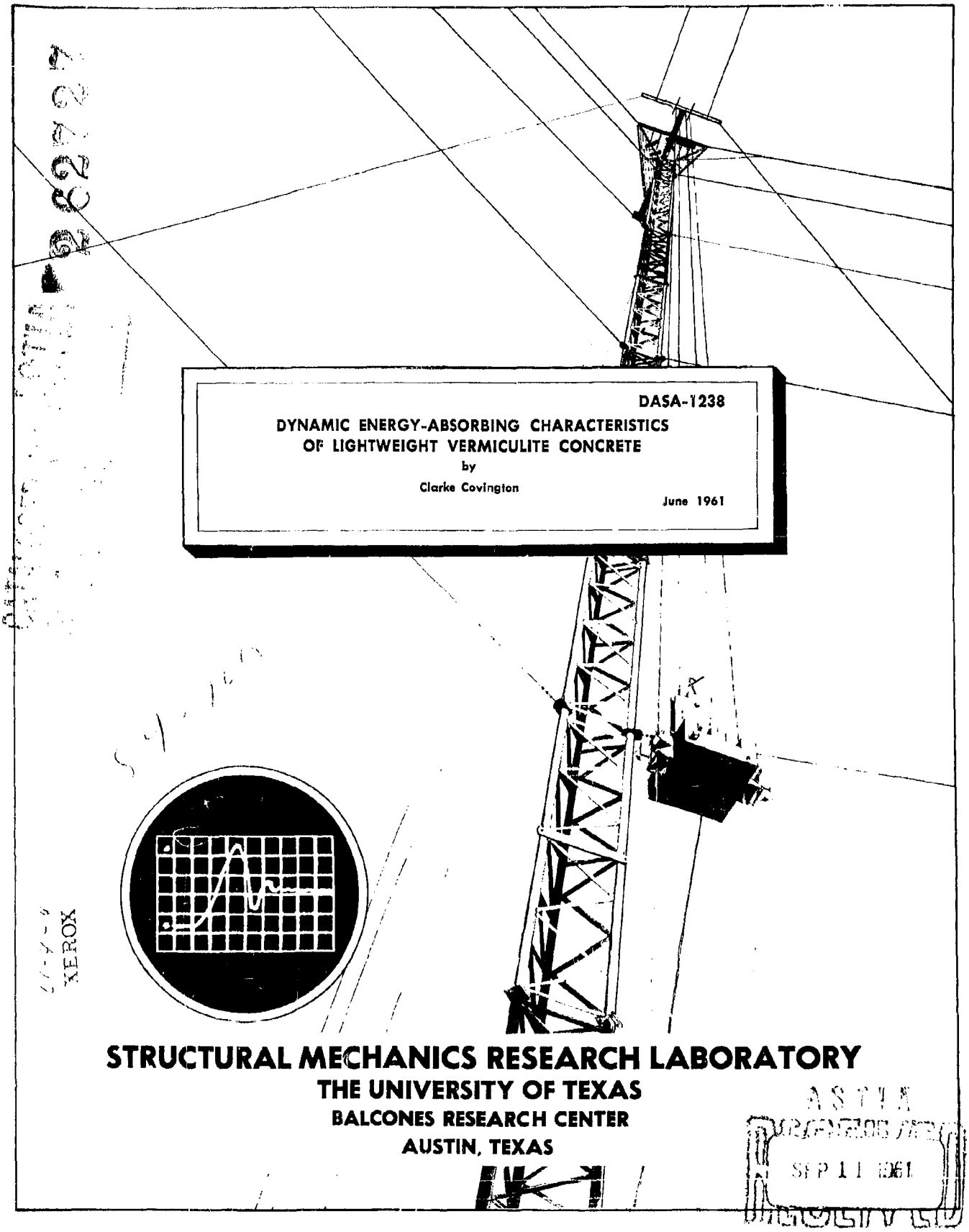

DASA-1238

DYNAMIC ENERGY-ABSORBING CHARACTERISTICS OF LIGHTWEIGHT VERMICULITE CONCRETE

by

Clarke Covington

June 1961

STRUCTURAL MECHANICS RESEARCH LABORATORY
THE UNIVERSITY OF TEXAS
BALCONES RESEARCH CENTER
AUSTIN, TEXAS

150

DASA-1238

UNCLASSIFIED

DYNAMIC ENERGY-ABSORBING CHARACTERISTICS OF LIGHTWEIGHT VERMICULITE CONCRETE

by

Clarke Covington

Prepared for

DEFENSE ATOMIC SUPPORT AGENCY

Contract DA 49-146-XZ-028

Nuclear-Weapons Effects Research Subtask 13.040

THE UNIVERSITY OF TEXAS

STRUCTURAL MECHANICS RESEARCH LABORATORY

Austin, Texas

June 1961

The Structural Mechanics Research Laboratory

is cooperatively operated by

The Engineering Mechanics and Civil Engineering Departments

at

The Balcones Research Center

University of Texas

Austin, Texas

PREFACE

A material which is suitable for use as a shock mitigator, or shock isolator, where only one extremely severe shock may be expected, must have certain specific basic properties. It must limit the force transmitted through it to some predetermined value which is essentially independent of the deformation which the material undergoes, even though this deformation is by normal standards extremely large. This limiting force should also be essentially independent of the rate of deformation. Other characteristics concerning fabrication and placing, stability under different environmental conditions, and availability may also be imposed on the material. Concretes made of lightweight aggregates and containing large amounts of air appear to have many of these desirable properties.

The present report concerns the cushioning properties of a lightweight concrete made with a vermiculite aggregate. It is expected that subsequent reports will be concerned with other cushioning materials, and other aspects of the problem of measuring the properties of cushioning materials.

J. Neils Thompson
Director
Structural Mechanics Research Laboratory
The University of Texas
Austin, Texas

June 1961

TABLE OF CONTENTS

TABLE OF CONTENTS
(Cont'd)

LIST OF FIGURES

LIST OF FIGURES
(Cont'd)

ABSTRACT

The dynamic energy-absorption characteristics of confined lightweight vermiculite concrete are presented in the form of stress-strain and stress-time curves. In addition, data are included which show the effects of impact velocity and impact mass weight on these characteristics. Stress-strain and energy-absorption characteristics are discussed.

A comparison is made between a dynamic and a static stress-strain curve for this material.

For a cement to vermiculite mix of one to eight, the initial peak crushing stress is between 420 and 570 psi, and the average crushing stress to 30 per cent strain is between 350 and 450 psi. The energy dissipated to 30 per cent strain is between 8.8 and 10.9 ft-lb/in.^{3}

INTRODUCTION

The value of building structures underground for protection has long been realized, and complete missile complexes and command posts are presently being built underground. These structures probably could be made strong enough to resist structural damage from even a very large applied force. However, the acceleration given to a structure would very likely damage the delicate equipment contained inside. In addition, differential movement might cause damage to the various necessary entrances to an underground structure. In order to minimize the possibility of this sort of damage, means for isolating structures from their surroundings are being sought.

On March 1, 1960, The University of Texas' Structural Mechanics Research Laboratory instigated for the Defense Atomic Support Agency a feasibility and an experimental study of materials and systems for the isolation of underground structures subjected to dynamic loads. Considerable work has been done by the Structural Mechanics Research Laboratory in the energy-absorption and shock-mitigating area dating back to the fall of 1953, when, at the request of the United States Army Quartermaster Corps, a survey of the present status of aerial-delivery practices and efficiency was undertaken. Since that time, studies have been made of the dynamic energy-absorbing properties of paper honeycomb,[1*] foamed plastics,[2, 3]

*Numbers indicate references as listed in the Bibliography.

wood,[4] and metal tubes and cans.[5] In addition, a limited study has been made of the energy-absorbing properties of 35 various materials ranging from rubber foam to aluminum honeycomb.[6]

SCOPE OF WORK

Background

The conclusions reached in a report[7] by the Department of the Navy Bureau of Yards and Docks are representative of several recent studies of the protection afforded an underground structure from a nuclear explosion. In general, some of those conclusions were (1) for large yield weapons (greater than 500 kiloton) and an uncushioned structure, survival probability is dependent upon the number of openings to the structure, (2) the probability of survival from air blast damage is essentially independent of depth of cover, and (3) the survival probability from ground shock effects is almost independent of depth of cover. In view of these conclusions, even though they may be subject to some argument, it appears necessary to cushion these structures in some manner.

A Stanford Research Institute report, Isolation of Structures from Ground Shock,[8] gives the final results of one of the 46 projects of Operation Plumbbob which included 24 test detonations at the Nevada Test Site in 1957. In this project, the benefit of a frangible backfill in isolating or protecting underground structures from violent motions in their vicinity was studied. Three-ft-diameter concrete pipes were positioned with their axes vertical and their tops covered with concrete slabs approximately 2 ft below ground level. Two pipes had their sides

and bottom lined one layer thick with glass quart gin bottles, bottom to top around the outside of the pipe. A third pipe had soil backfilled directly against the pipe. The peak accelerations of these structures produced by shear forces exerted against their sides were reduced by the frangible backfill to values less than 26 per cent of those the structures would have experienced if they had made contact with the soil.

From this project, the general recommendation was made that theoretical, laboratory, and field test studies of special backfills, or cushioning materials, should be undertaken. One of the specific recommendations was that laboratory tests be performed to determine the appropriate properties of promising materials, including compressive stress-strain characteristics under both static and dynamic conditions.

Since the production and propagation of ground shock is not a well-understood phenomenon, in this study no particular attempt is made to take into account the loading characteristics of a nuclear shock wave. Instead, it will be limited to the general energy-absorption characteristics of a cushioning material.

Preliminary Investigation

In a preliminary investigation, the stress-strain characteristics of several types of lightweight concrete were studied. These included concrete made from four grades of vermiculite, two grades of perlite, and two grades of pumice. Of these materials, the vermiculite concretes

exhibited the best cushioning properties.* The crushing stress of the perlite concretes was about twice that of the vermiculite, and the crushing stress of the pumice concrete was too high to consider it as a cushioning material. Static compression tests were made with a confining pipe filled with each loose aggregate. Uncemented aggregate, even though confined, does not appear to be very effective as an energy absorber. The energy-absorbing capability of lightweight concretes apparently depends upon the work required to fracture the cement binder. The aggregate itself probably absorbs very little energy. This suggests that a cement paste with a large volume of entrapped air would be just as effective as an energy absorber as the lightweight aggregate concretes. Of the vermiculite aggregates, the No. 3 aggregate, called vermiculite plaster aggregate, appeared to have the best stress-strain characteristics for cushioning when mixed to make a lightweight concrete.

Object

The object of this study was to investigate the cushioning characteristics of lightweight concrete made with vermiculite plaster aggregate by analyzing stress-strain and stress-time relationships made under varying conditions.

Related Project

A closely-associated investigation was conducted by Shield[9] at the Structural Mechanics Research Laboratory to determine the shock-

*As defined later in the chapter "Discussion of Cushioning Principles."

mitigating properties of lightweight vermiculite concrete. Shield's study involved firing a 25-lb, 4-in. -diameter steel projectile into a heavy mass cushioned with lightweight concrete. An accelerometer mounted on the heavy mass recorded the acceleration of the system. Shield's work extended into a higher range of impact velocities that were not feasible with the drop tests.

DISCUSSION OF CUSHIONING PRINCIPLES[1]

Stress-Strain Characteristics

The stress-strain curve for a material assembles the most fundamental items of information concerning the suitability of that material for use as an energy absorber into one picture. No other single curve provides as much information concerning the energy-dissipation and energy-absorption characteristics of a material.

For the convenience of those not familiar with the definitions of stress and strain as they apply to the cushioning problem, these definitions are repeated here.

Stress is the value obtained by dividing the load applied normal to the face of the cushion by the face area of the cushion. Stress is then the normal load per unit of face area with pounds per square inch the convenient unit of measure here. Strain is the value obtained by dividing the vertical deformation of the cushion by the original depth. It is a dimensionless number and never exceeds a value of 1.0 or 100 per cent. During the deformation of a cushion, there exist corresponding values of stress and strain at each instant during the interval of deformation. If these corresponding stress and strain values are plotted, the so-called stress-strain curve is obtained. The area under this curve represents energy absorbed in ft-lb per cubic inch.

The stress-strain curve provides the following information concerning a material intended for use as a cushioning material:

1. The maximum stress which would be encountered in crushing the material. Knowledge of this stress value permits

the designer to adjust the face area of the cushion or to select a suitable material in order to limit the maximum acceleration to any selected value.

2. The shape of the stress-strain curve--the ideal curve for energy absorption, but not necessarily the best for cushioning, is one in which the stress remains constant at all strains, i.e., a rectangular stress-strain curve extending to large values of strain.

3. The maximum strain to which the cushion material may be deformed without inducing excessively high cushion stresses and associated accelerations on the protected items

4. The energy dissipated* per unit volume of cushion--this energy value permits determination of the actual volume of cushioning required to protect a structure. The dissipated energy per unit cushion volume is equal to the area under the stress-strain curve out to whatever strain is desired when this area is expressed in energy units, as shown in Fig. 2.

Energy Dissipation

The energy dissipated by a material depends upon two factors:

---

*In the past, there has been some carelessness surrounding the use of the terms "energy absorbed" and energy dissipated." For most cushioning systems, a certain amount of energy which is absorbed by the cushion at initial impact is retained as elastic energy. This energy may be returned to the cushioned mass in the form of rebound. The dissipated energy of an impact is equal to the total energy absorbed minus the elastic energy, or rebound energy. As shown in Fig. 1, the dissipated energy is represented on a stress-strain curve by the area enclosed by the curve and the x-axis. The energy absorbed is represented by the area under the stress-strain curve out to a vertical line drawn down from the point of maximum strain. For strain values less than that where rebound starts to occur, dissipated energy and absorbed energy are equal.

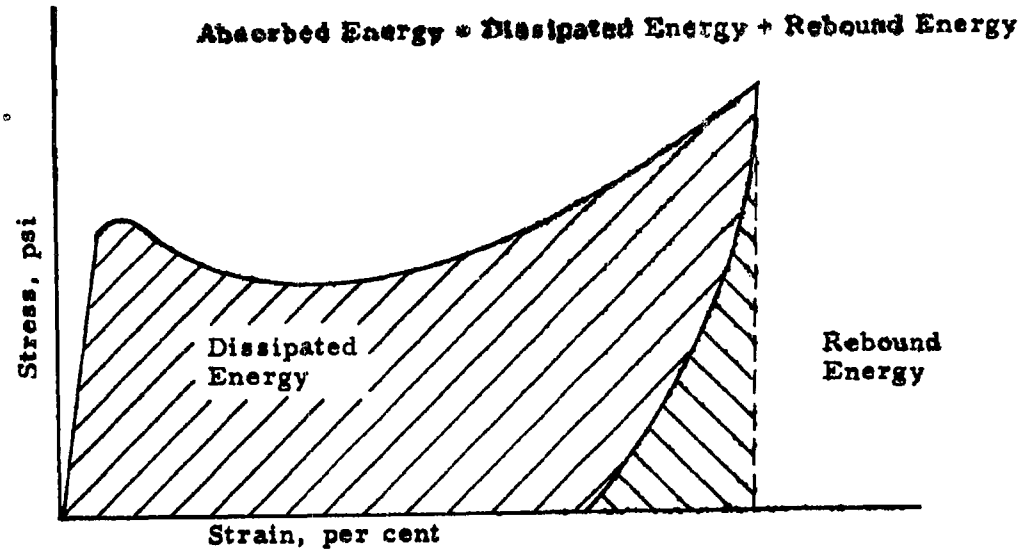

Fig. 1. Typical Stress-Strain Curve Showing Absorbed Energy, Dissipated Energy, and Rebound Energy.

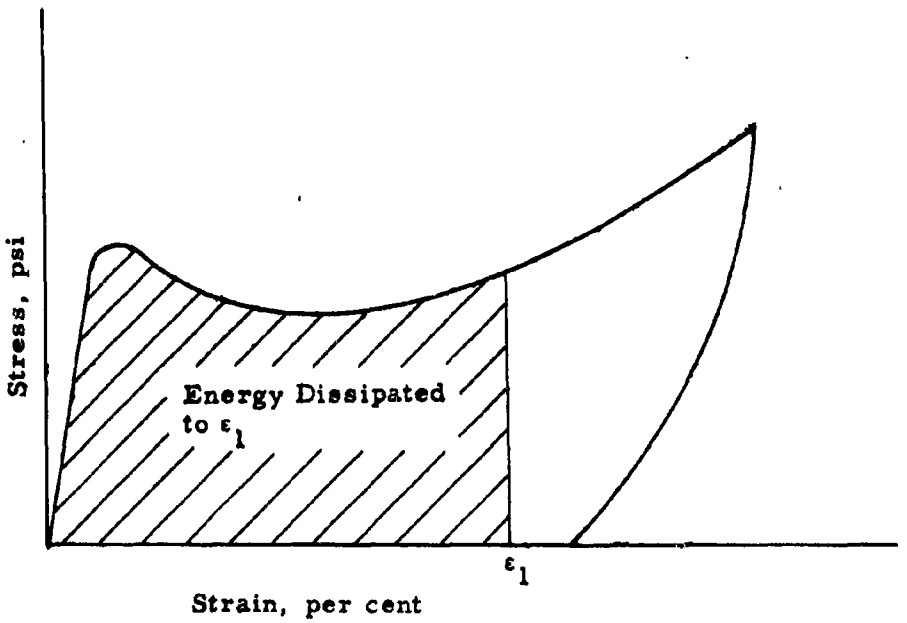

Fig. 2. Typical Stress-Strain Curve Showing Energy Dissipated to a Particular Strain.

(1) the deformation of the material, and (2) the forces in the material during the deformation. The amount of energy absorbed is the product of the average force and the deformation. For any given cushioning problem, it has been customary to assume a maximum force to which the protected item can be subjected without producing damage. Thus, two requirements normally must be met by the cushioning system. First, a certain amount of energy must be dissipated. Second, the maximum force must be kept at or below a given maximum value. These conditions are best met by the "ideal" cushion having a rectangular force-displacement curve as shown in Fig. 3.

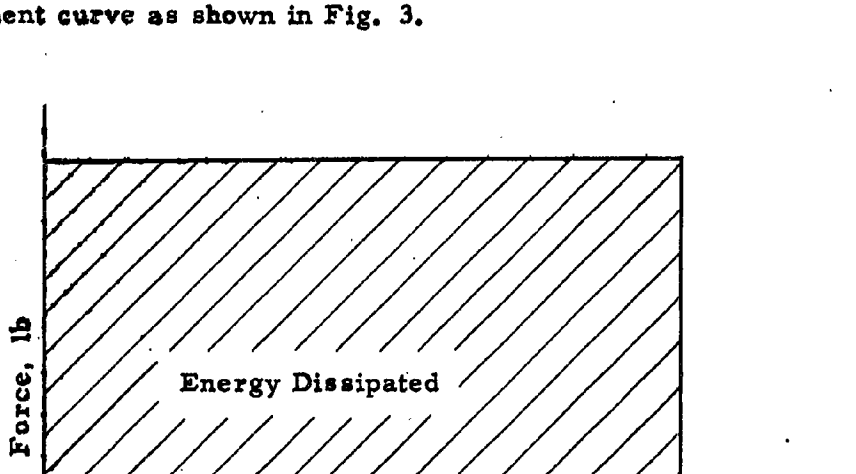

Fig. 3. Ideal Rectangular Force-Displacement Curve.

With this ideal material, a constant cushioning force is maintained throughout the impact, and the energy is dissipated with a minimum of displacement. The area under the force-displacement curve, when

expressed in ft-lb, is equal to the energy dissipated.

To put the characteristics of materials on a basis which will allow them to be readily compared to the characteristics of other materials, force-displacement curves are converted to stress-strain curves, where the stress

$$\sigma = \frac{F}{A} \qquad \text{- - - - -} \qquad (1)$$

is the force, F, per unit area, A, of the cushioning pad, and the strain

$$\varepsilon = \frac{d}{t} \qquad \text{- - - - -} \qquad (2)$$

is the deformation, d, of the specimen per unit initial thickness, t. The areas under the stress-strain curves represent the energy per unit volume of cushion as contrasted to the force-displacement curve which gives the total energy for the specimen. These relations may be seen for the case of a rectangular force-displacement (and thus stress-strain) curve.

$$\text{Total energy } E_n' = F \cdot d = \text{Area under the F - d curve in ft-lb} \qquad (3)$$

Dividing by the specimen volume

$$\frac{E_n'}{\text{Specimen volume}} = E_n = \frac{F \cdot d}{A \cdot t} = \frac{(F)}{(A)} \frac{(d)}{(t)} = \sigma \cdot \varepsilon$$

or,

$$E_n = \sigma \cdot \varepsilon = \text{Area under the stress-strain curve.}$$

Here, E_n is the energy per unit volume. The above equations are true only if the force, F, and stress, σ, are expressed as average values, or if the force-deflection curve is rectangular as shown in Fig. 3. In all cases, the energy per unit volume is given by

$$E_n = \int_0^{\varepsilon_1} \sigma \cdot d\varepsilon \qquad \text{- - - -} \qquad (4)$$

EXPERIMENTAL PROCEDURE

Materials

Vermiculite aggregate. Vermiculite is a micaceous mineral that exfoliates when heated or subjected to certain chemical reactions. It is a hydrated magnesium-aluminum-iron silicate. The No. 3 vermiculite aggregate has a density of 7 to 10 lb per cu ft, and is sized so that virtually all of the material passes a No. 8 sieve and all of it is retained on a No. 50 sieve. This material was specified as Vermiculite Plaster Aggregate and was obtained from the Texas Vermiculite Company of Dallas, Texas.

Cement. The cement used was made by the Alamo Cement Company of San Antonio, and was specified as Alamo Type 1 Portland Cement.

Admixture. The admixture was a neutralized vinsol resin made by the Hercules Powder Company.

Preparation of Lightweight Concrete Specimens

The lightweight concrete used in this investigation was prepared in the Civil Engineering Laboratory of The University of Texas. The concrete was mixed in a Lancaster mixer and poured into standard 6-in.-diameter, 12-in.-long test cylinders. All the concrete was proportioned with a water to cement to vermiculite volume ratio of 3.08:1:8. The concrete was mixed in batches of 2 cu ft of vermiculite, 0.25 cu ft of cement, and 0.77 cu ft of water to which 100 gm of a neutralized vinsol resin admixture was added to make an easily workable mixture.

This amount of admixture entrained 20 to 30 per cent air in the concrete, as measured with a Washington Air Meter. The mixture contained an indicated 8 per cent entrained air with no admixture, due to the "spongy" nature of the aggregate. Thus, the air content of the paste must have been somewhat less than the meter indicated.

The water content of the mix was determined initially by slowly adding water to the mix until a consistency suitable for pumping was reached. In general, this was a consistency that gave a slump of approximately 8 inches. Thereafter, this initially-determined amount was kept constant.

After being poured, the specimens were cured in the forms for two days and then taken out and placed in a 100 per cent humidity room. After curing in the 100 per cent humidity room for two weeks, the specimens were sealed wet in plastic bags to give a total curing time of at least 30 days before testing to minimize curing effects. After curing 30 days, the concrete specimens had a density of 47 to 53 lb/cu ft. The tests were all made with the concrete saturated to simulate field conditions.

Although a special effort was made to control the concrete mix to insure uniformity of test specimens, the density of the concrete specimens varied between 47 and 53 lb/ft^3 from batch to batch. This variance is probably responsible for a large part of the "scatter" in the data that increases the difficulty of interpretation. The concrete mix seemed to be very sensitive to mixing procedure, and, during the latter part of the project when the mixing technique was perfected, the densities did not vary as much.

Confining System

All the dynamic stress-strain and stress-time measurements were made with the specimens confined laterally. The 6-in. x 12-in. cylinders were taken from the sealed plastic bags as needed and sawed into the required thicknesses with a hacksaw. The faces of the test cylinders were made perpendicular to their sides by placing the specimens in a 6-in.-diameter form and scraping the faces until they were plane. When prepared for a test, the specimens were confined in 6-in. inside diameter x 6-1/2-in. or 12-1/2-in.-long steel pipes with a 1/4-in.-thick wall. An aluminum plate 1/2-in. thick was placed on top of each specimen, and then a 4-in.-i.d. steel pipe was placed on top of each plate. The pipes with the aluminum plates formed a plunger for crushing the material inside the confining tubes without allowing the impacting mass to also strike the tubes. When the 6-1/2-in.-long confining steel cylinders were used, 4-in.-long plunger pipes were used. For the 12-1/2-in.-long confining cylinders, 7-1/2-in.-long plunger pipes were needed. As many as four 6-1/2-in. or three 12-1/2-in.-long confining cylinders were impacted in a single test. The total weight of one aluminum plate and steel pipe plunger system was about 5 lb for the short plunger and 8 lb for the longer one as compared to the impact mass weight of 236 to 611 pounds. A diagram of the confining systems is shown in Fig. 4.

Static compression tests were made using the same confining systems.

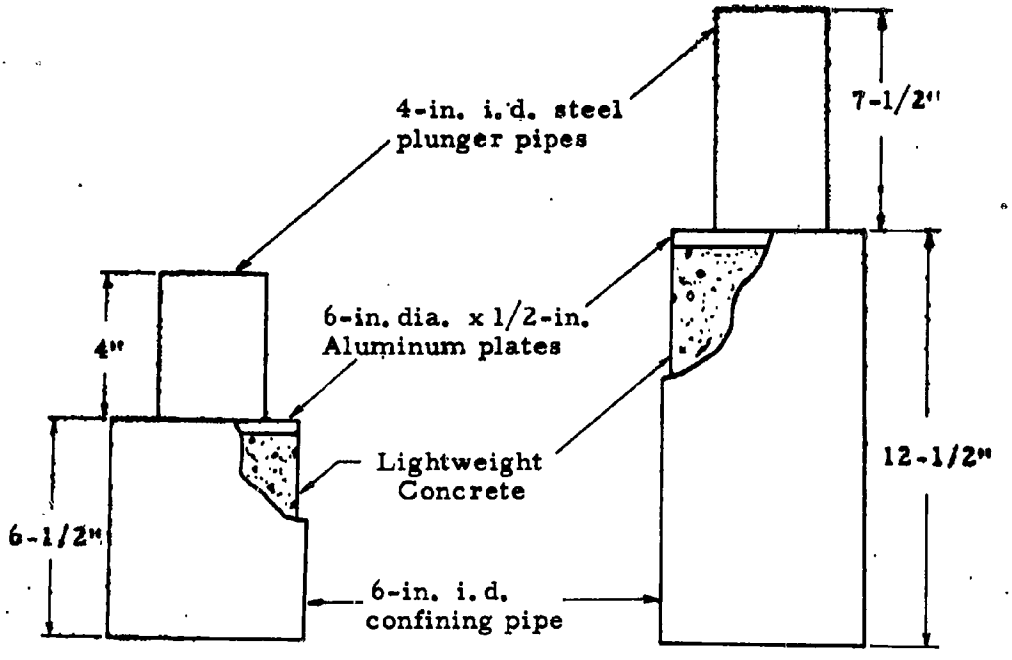

Fig. 4. Diagram of Confining Systems.

Drop Facility

Force-displacement. The stress-strain and stress-time measurements were made using the Structural Mechanics Research Laboratory 275-ft drop-tower facility shown in Fig. 5. A fixed force plate was used for measuring the force of impact. The force plate is supported by four dynamometers, each of which has four type C-1 SR-4 strain gages mounted on it. The strain gages are connected in a bridge circuit, and the output of this bridge is applied to the y-axis of two cathode-ray oscilloscopes.

Deformation, or axial compression of the confined test specimen, is measured by means of wiper arms attached to the impacting mass, and a resistance slide-wire arrangement that is supported independently of the specimen. The wiper arm contacts are mounted on thin sheets of phenolic-resin-impregnated material which are attached to the mass as shown in Fig. 5. These contacts enter two displacement transducer funnels, in which resistance slide wires are mounted, as the falling mass approaches the specimen. The slide wires are arranged in a bridge circuit and provide a voltage gradient such that the open-circuit voltage is proportional to the position of the contact on the wire. The bridge output is applied to the x-axis of one of the cathode-ray oscilloscopes.

Force-time. The x-axis of the other oscilloscope reads out elapsed time, and it is triggered when the falling mass closes a wire switching arrangement placed a short distance above the test specimen.

Calibration. The force-measuring circuit is calibrated by switching shunt resistors rapidly across one arm of the strain-gage bridge. For

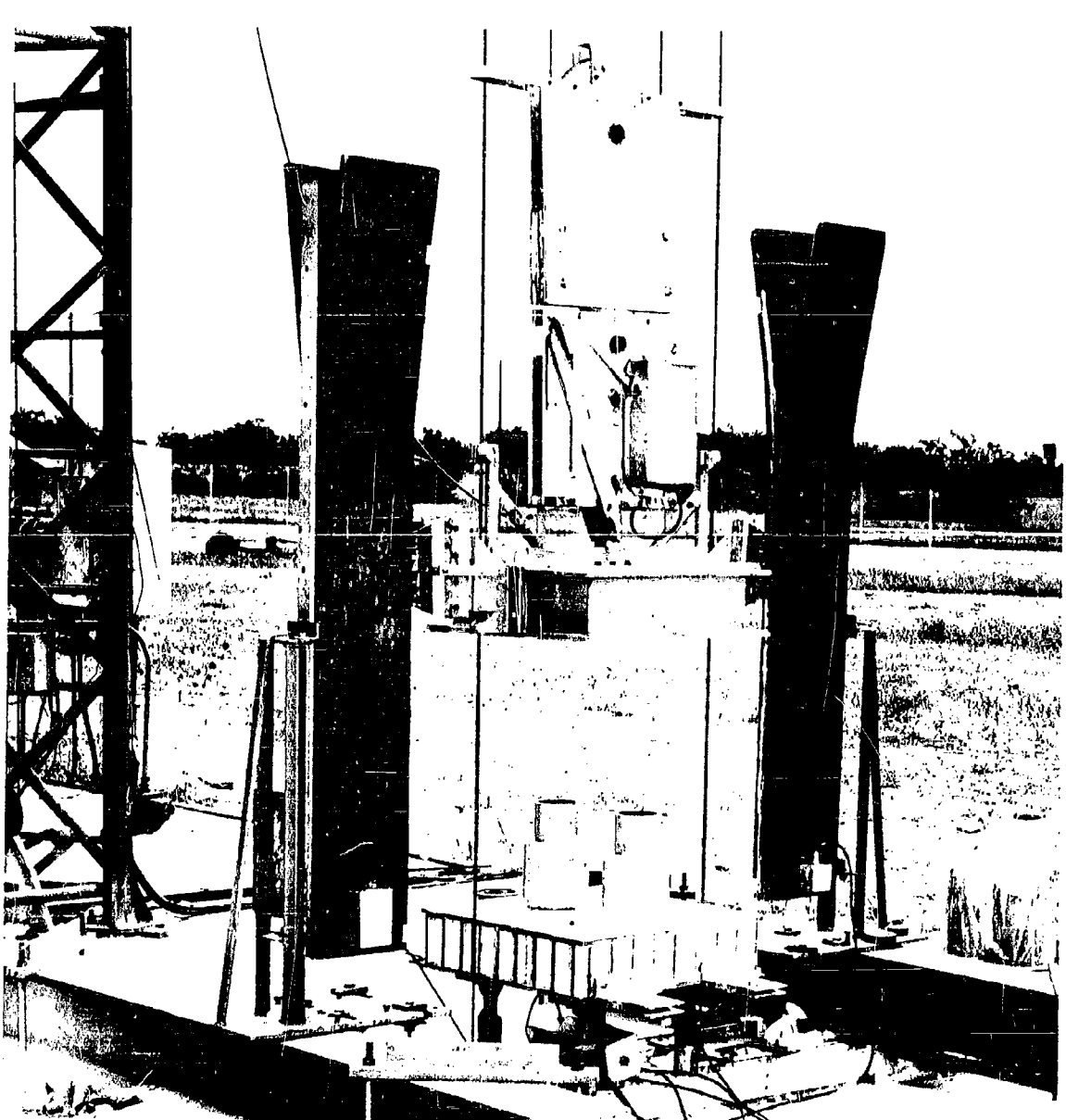

Fig. 5. 275-ft Drop Tower Force-Deformation Measuring Devices.

displacement calibration, contacts with precisely-known spacing were placed temporarily in the displacement transducer funnels. The calibrations and records were recorded photographically on the same film by double-exposure. Typical force-deformation and force-time photographs are shown in Figs. 6 and 7. Calibration marks appear as small dots on the pictures.

To check the accuracy of the data, the area under each force-time curve, which represents the total impulse applied to the specimen, was integrated with a planimeter. This impulse will be equal to the change in momentum of the falling mass if the force and displacement calibrations are correct. This impulse-momentum check indicated that the calibration factors are correct. Although it is not as sensitive a check as the impulse-momentum method, an energy balance was made in which the available kinetic energy of the falling mass at impact was compared with the total energy absorbed by the cushioning material. This method also showed that the data were essentially correct.

Data Reduction

The photographic records obtained from the two oscilloscopes were plots of force vs deformation and force vs time. Force was converted to stress by dividing it by the total cross-sectional area of the impacted specimen. The deformation was divided by the original height of the test specimen to obtain the strain. The oscillogram records were reduced and plotted directly onto graph paper, with scales properly adjusted, by using a Telecomputing Corporation Telereader and a Moseley Autograf x-y plotter.

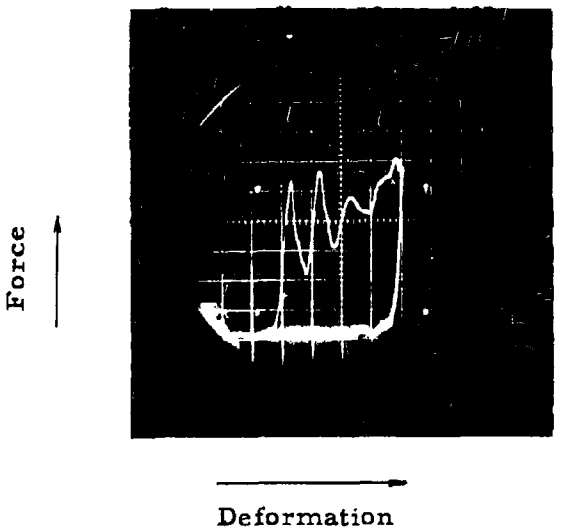

Fig. 6. A Typical Force-Deformation Curve for Vermiculite Concrete.

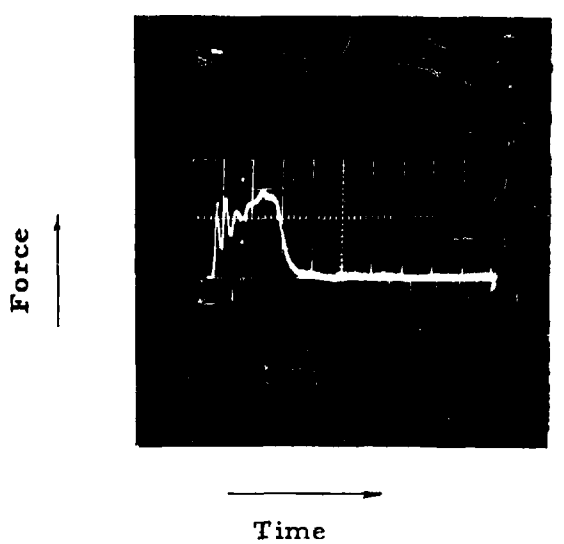

Fig. 7. A Typical Force-Time Curve for Vermiculite Concrete.

DISCUSSION OF RESULTS

Figs. 8 through 34 show the dynamic stress-strain and corresponding stress-time curves for 33 drop tests onto confined vermiculite concrete. For these tests, the impacting mass weight was varied between 236 lb and 611 lb, and the impact velocity was varied between 10.8 fps and 60 fps. During all tests, the energy input to the lightweight concrete was held constant at 13 ft-lb per cubic inch of concrete.

Stress-time relationships were recorded to observe the effects of impact velocity change and impact mass weight change on the stress rise time.

The initial peak crushing stress in this velocity range is between 420 and 570 psi, and the average crushing stress to 30 per cent strain is between 350 and 450 psi. The energy dissipated to 30 per cent strain is between 8.8 and 10.9 ft-lb/cu inch. Average crushing stress and energy dissipated were measured to 30 per cent strain because the stress begins to rise rapidly, or the material "bottoms," at strains above 30 to 35 per cent. Because of this, for a displacement of 1 ft, about 3 ft of material is needed.

The stress-strain and stress-time curves presented are averages of three taken under identical conditions. A summary of data is included in the Appendix in Table I.

Static Compression

Fig. 8 shows a static stress-strain curve plotted along with a low-

velocity, 15.3 fps, dynamic stress-strain curve for comparison. The static curve has an initial peak that is about half that of the dynamic curve, and the bottoming portion of the static curve parallels the dynamic curve, but with only about two-thirds of the stress value. The wiggles in the dynamic curves after the initial peak, and some of the magnitude of the first peak, probably were caused by the instrumentation.[10]

Effect of Impact Velocity

Figs. 9 through 22 show the dynamic stress-strain and corresponding stress-time curves for vermiculite concrete when the impact velocity is varied from 10.8 fps to 60 fps in 7 steps. The initial peak stress and average stress out to 30 per cent strain for each of the 7 points are plotted against impact velocity in Fig. 23. The average stress was calculated by measuring the area under the stress-strain curves out to the 30 per cent strain line, expressing this area in energy units, in.-lb per cubic in., and then dividing this area by 0.30-in. per inch. The initial peak stresses appear to increase by about 30 per cent in the velocity range 10 fps to 60 fps, and the average crushing stresses seem to have a definite upward trend, but not as much as the initial peaks. Fig. 24 shows that the energy absorbed to 30 per cent strain increases with impact velocity with the same slope as the average crushing stresses. This is necessarily so, because of the procedure followed in calculating the average crushing stress from the energy absorbed. The stress-time curves show that there is no appreciable change in rise time with an increase in impact velocity. Each initial peak appears at about 0.5-millisecond after impact.

Effect of Impact Mass Weight

Figs. 25 through 32 show stress-strain and stress-time curves for a constant impact velocity and 4 different mass weights varying from 236 to 505 pounds. A fifth mass weight, 611 lb, has already been shown in Figs. 13 and 14. The plot of initial peak stresses and average stresses to 30 per cent strain vs impact mass weight, shown in Fig. 33 shows no definite effect on stress in the mass weight range 236 lb to 611 pounds. The energy absorbed per unit volume of material to 30 per cent strain, Fig. 34, is unaffected by mass weight change in this range, also. The stress-time curves show that there is no appreciable change in rise time with change in impact mass weight.

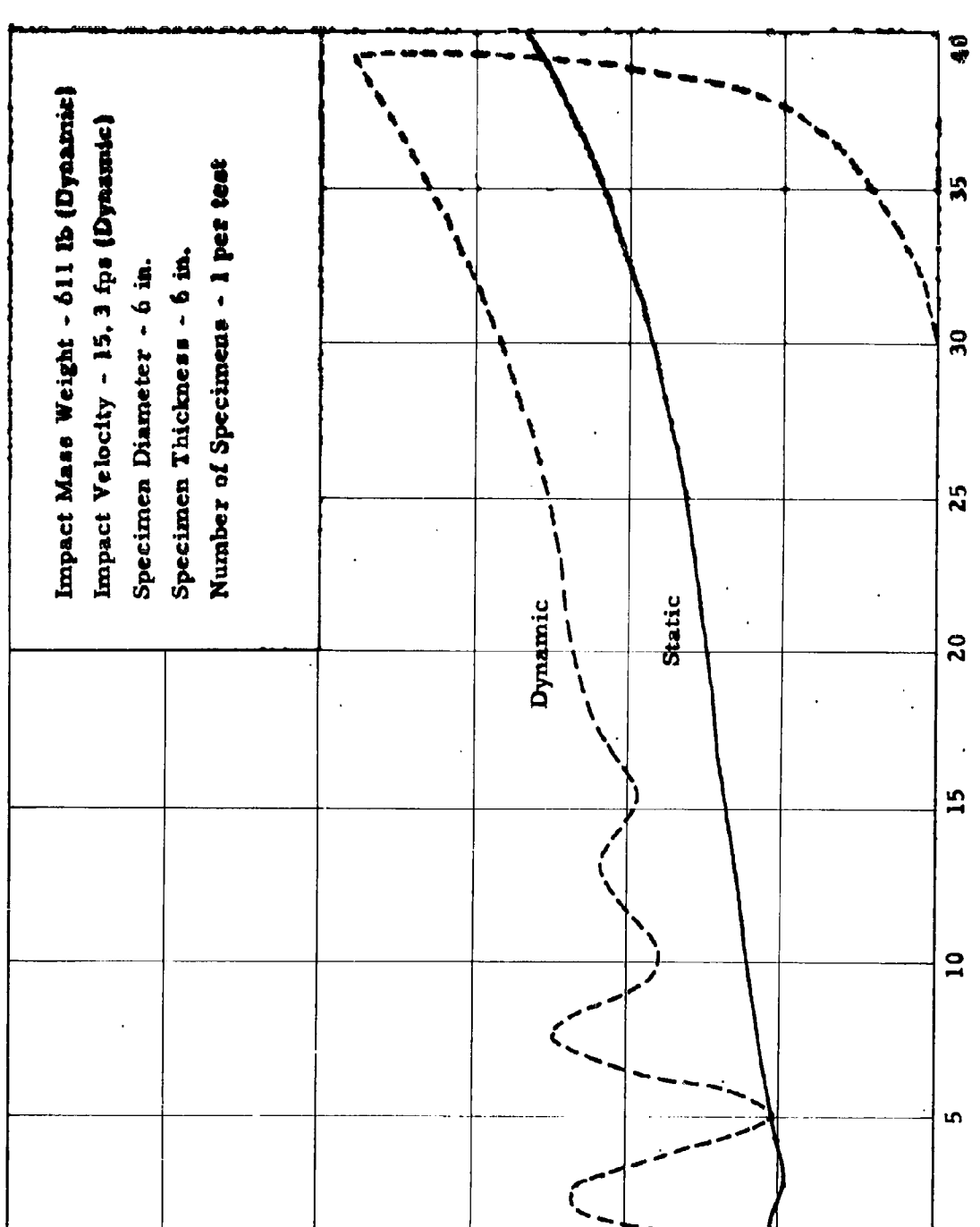

Fig. 8. Static and Low Impact Velocity Dynamic Stress vs Strain Curves.

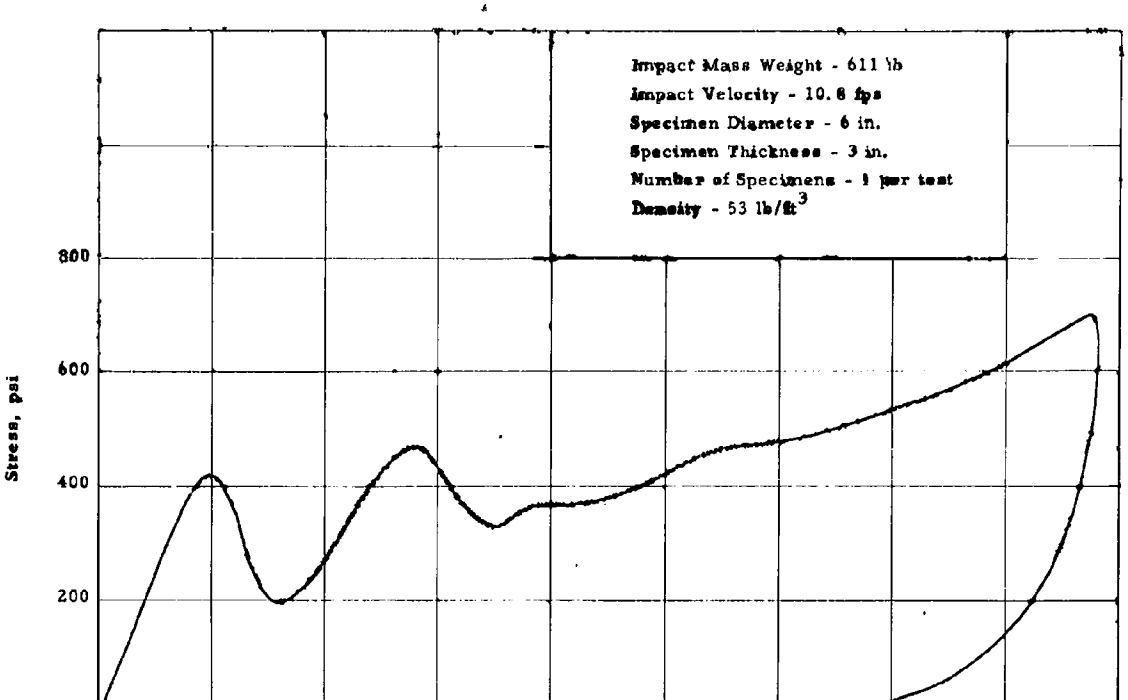

Fig. 9. Dynamic Stress vs Strain Curve at 10.8 fps.

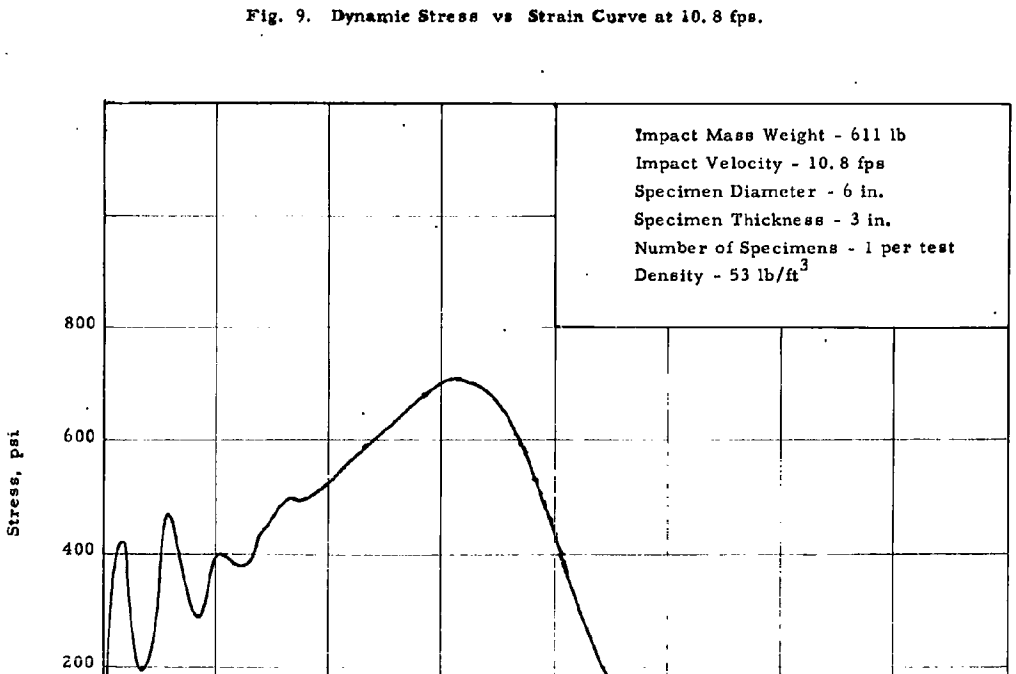

Fig. 10. Dynamic Stress vs Time Curve at 10.8 fps.

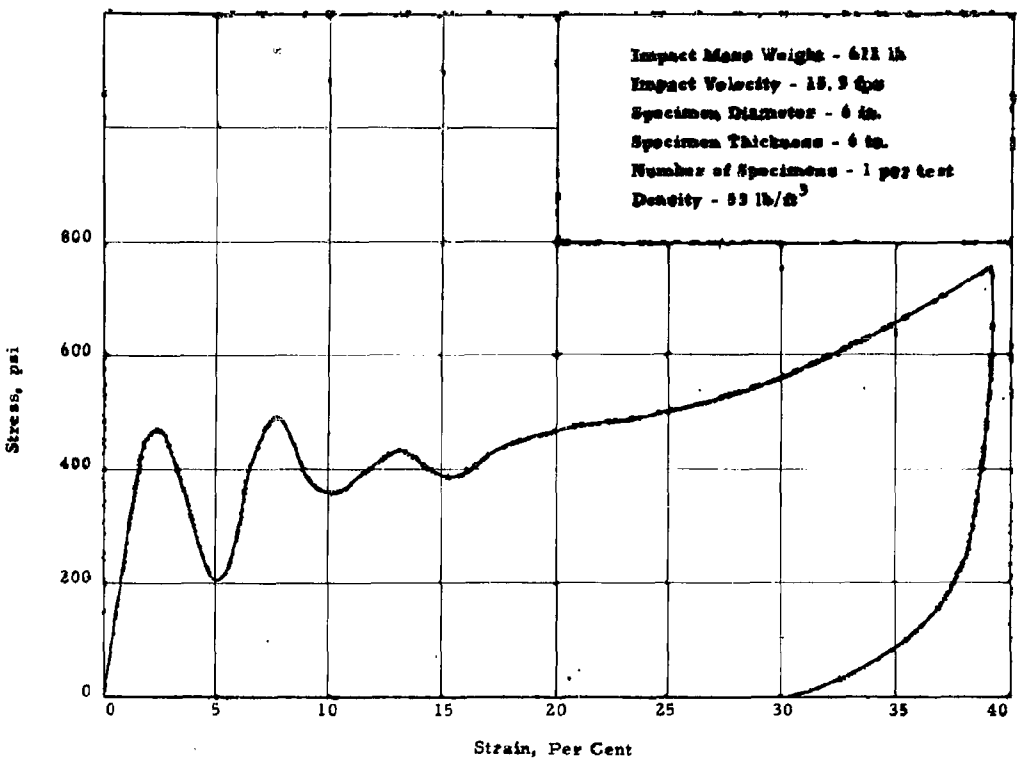

Fig. 11. Dynamic Stress vs Strain Curve at 15.3 fps.

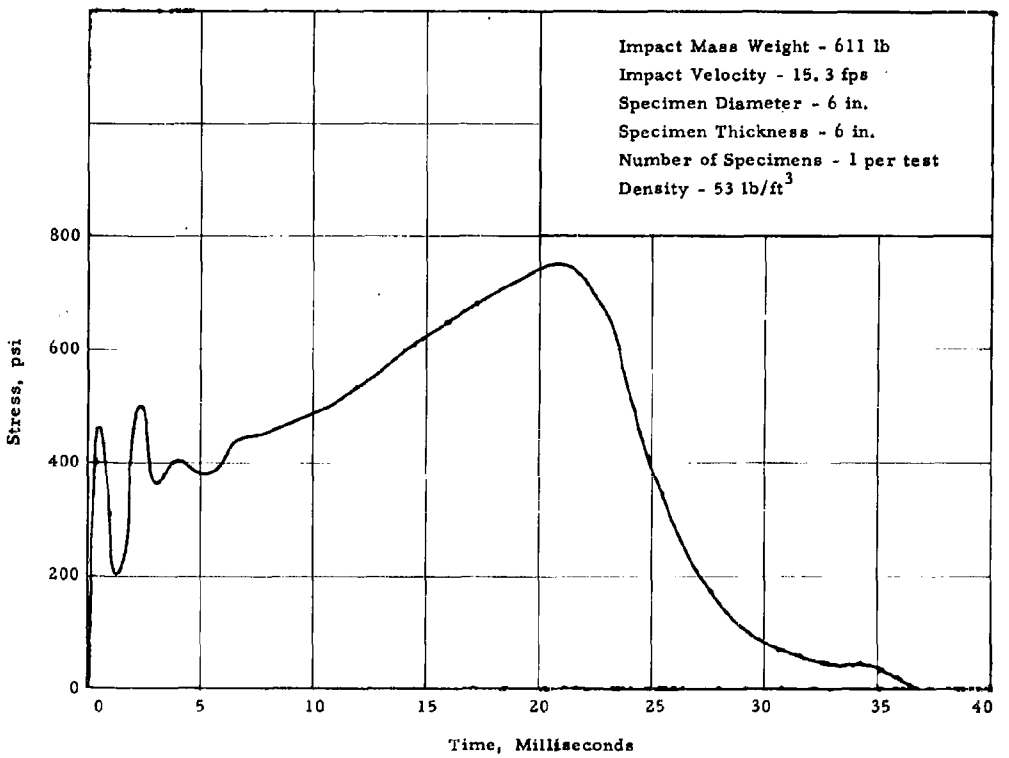

Fig. 12. Dynamic Stress vs Time Curve at 15.3 fps.

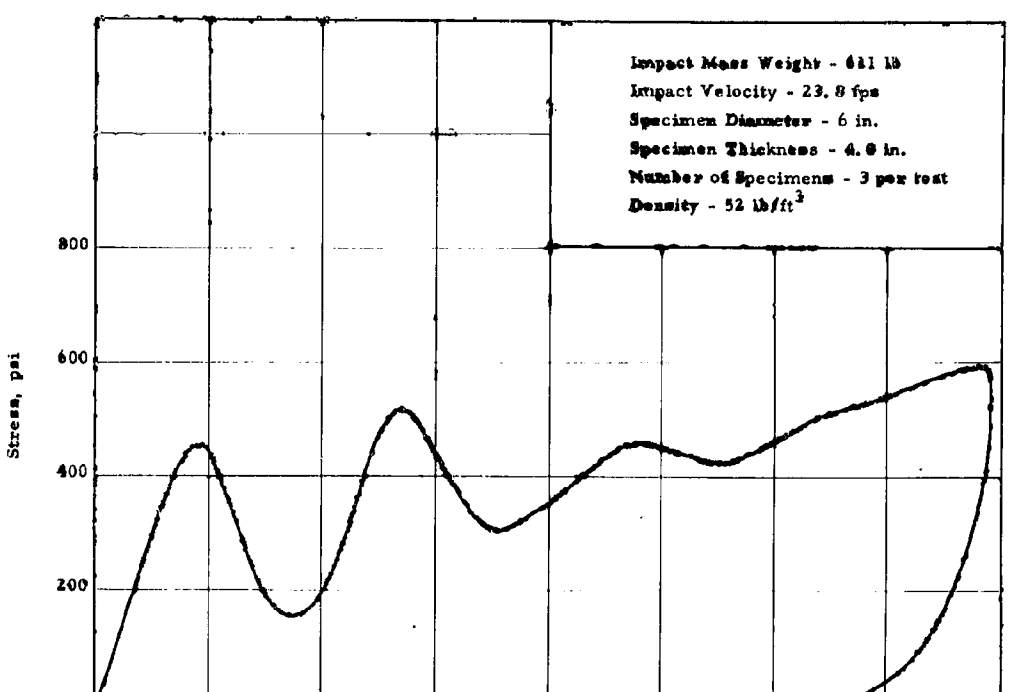

Fig. 13. Dynamic Stress vs Strain Curve at 23.8 fps.

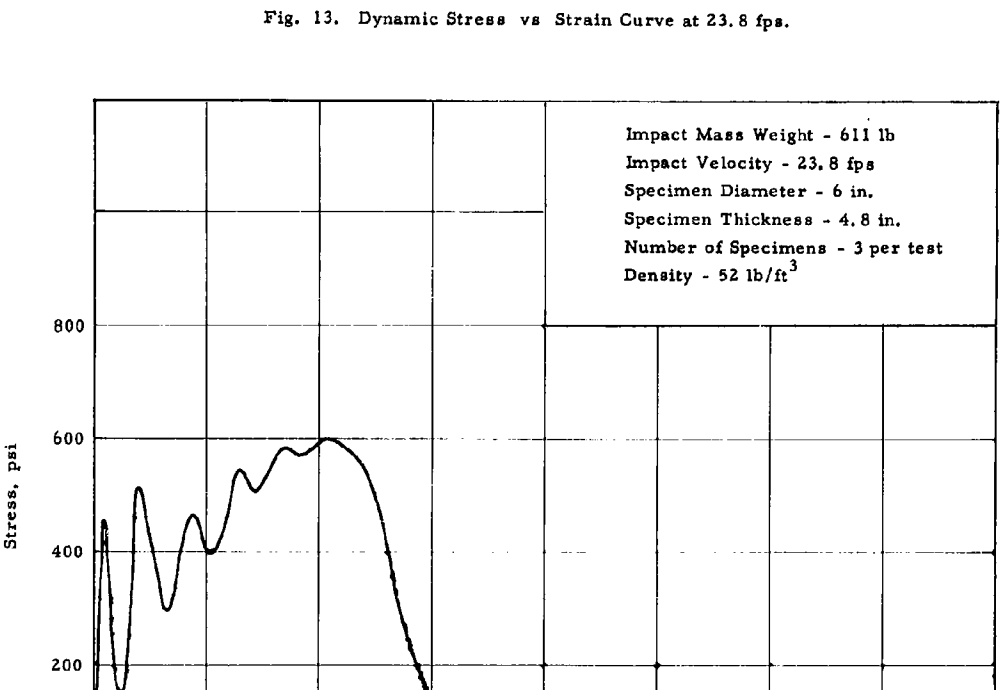

Fig. 14. Dynamic Stress vs Time Curve at 23.8 fps.

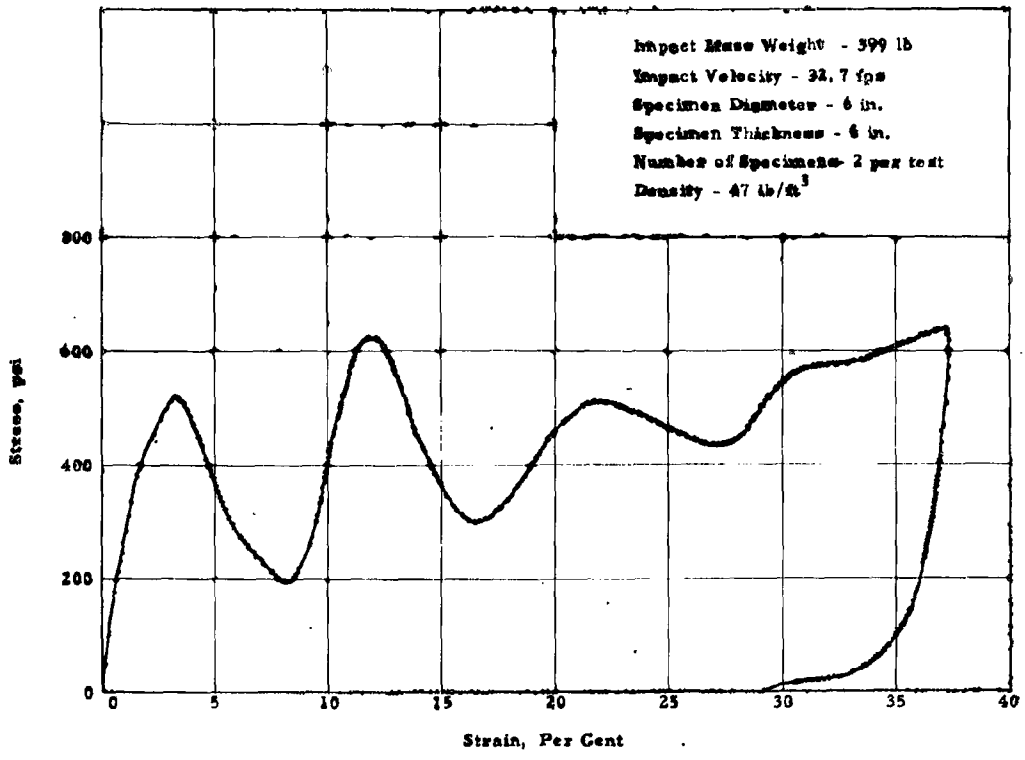

Fig. 15. Dynamic Stress vs Strain Curve at 32.7 fps.

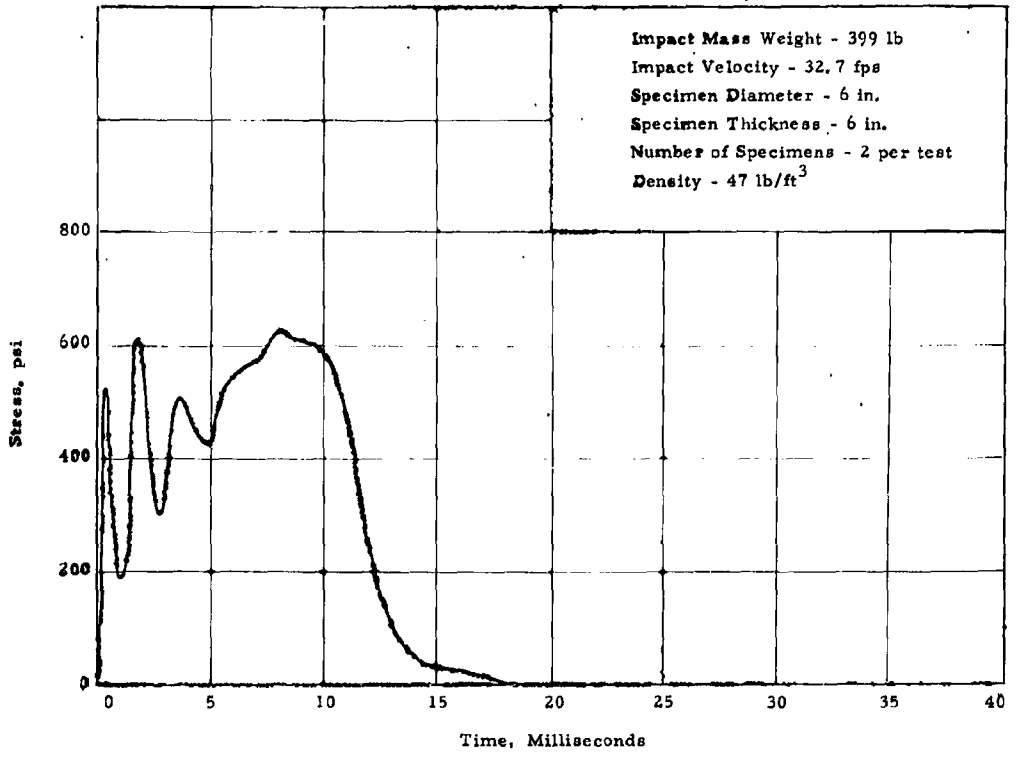

Fig. 16. Dynamic Stress vs Time Curve at 32.7 fps.

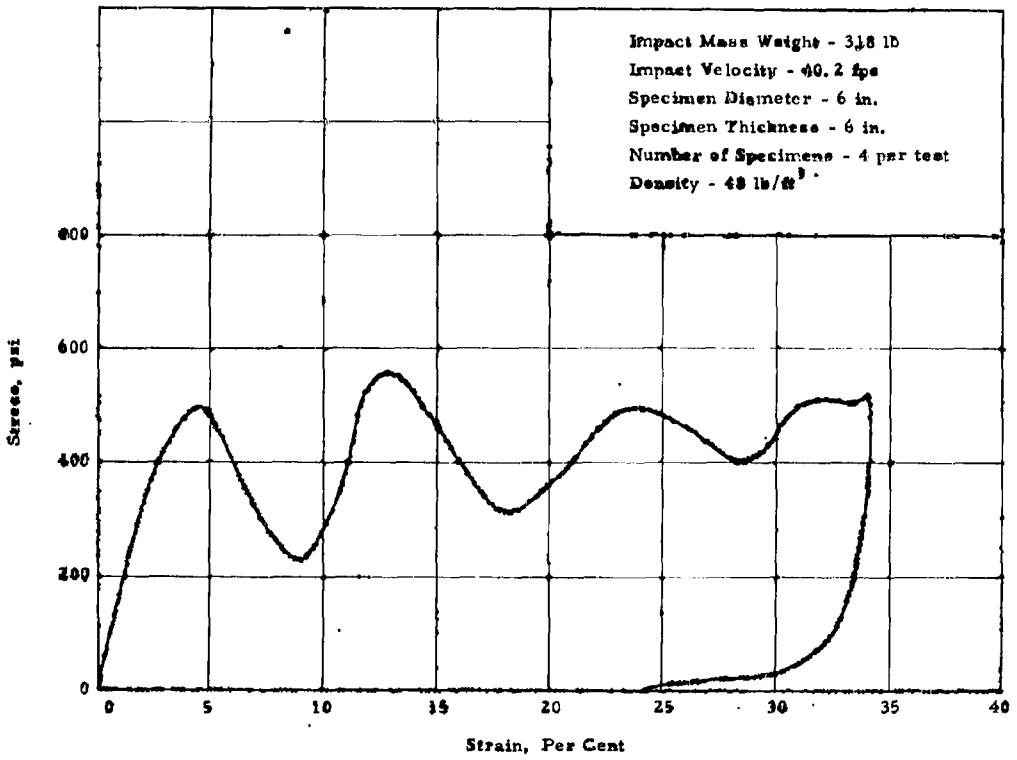

Fig. 17. Dynamic Stress vs Strain Curve at 40.2 fps.

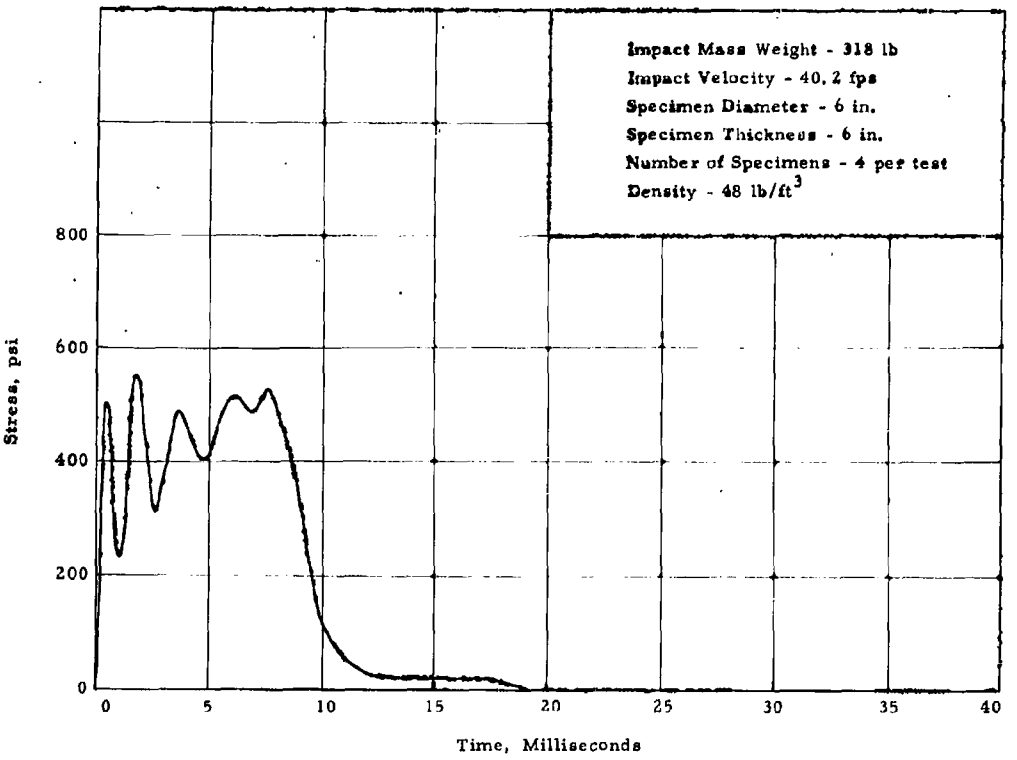

Fig. 18. Dynamic Stress vs Time Curve at 40.2 fps.

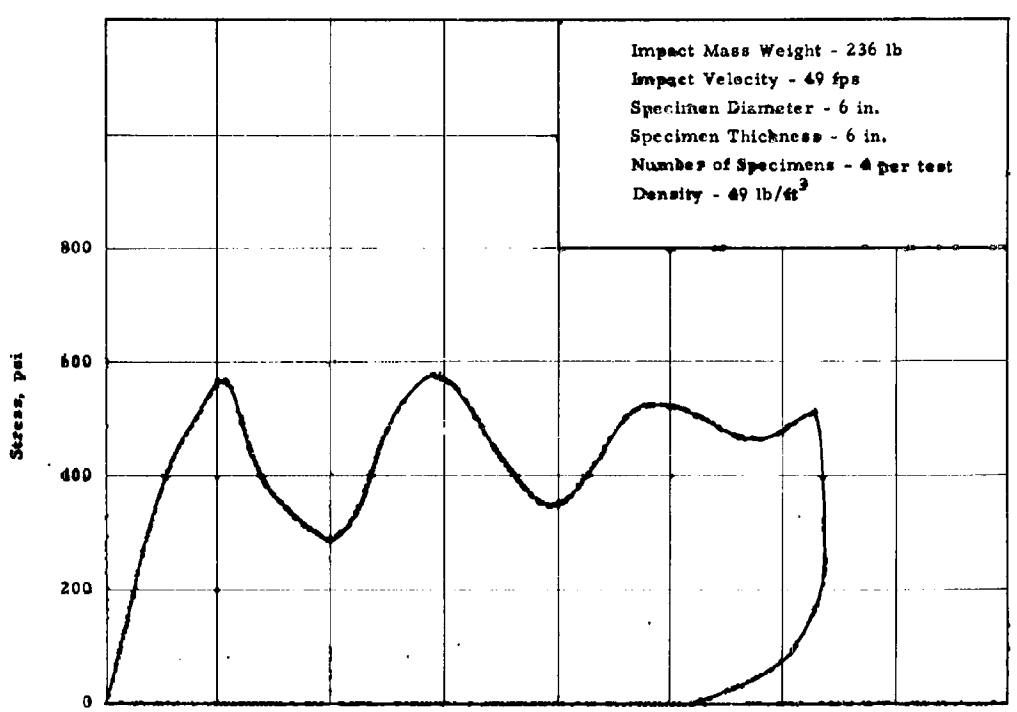

Fig. 19. Dynamic Stress vs Strain Curve at 49 fps.

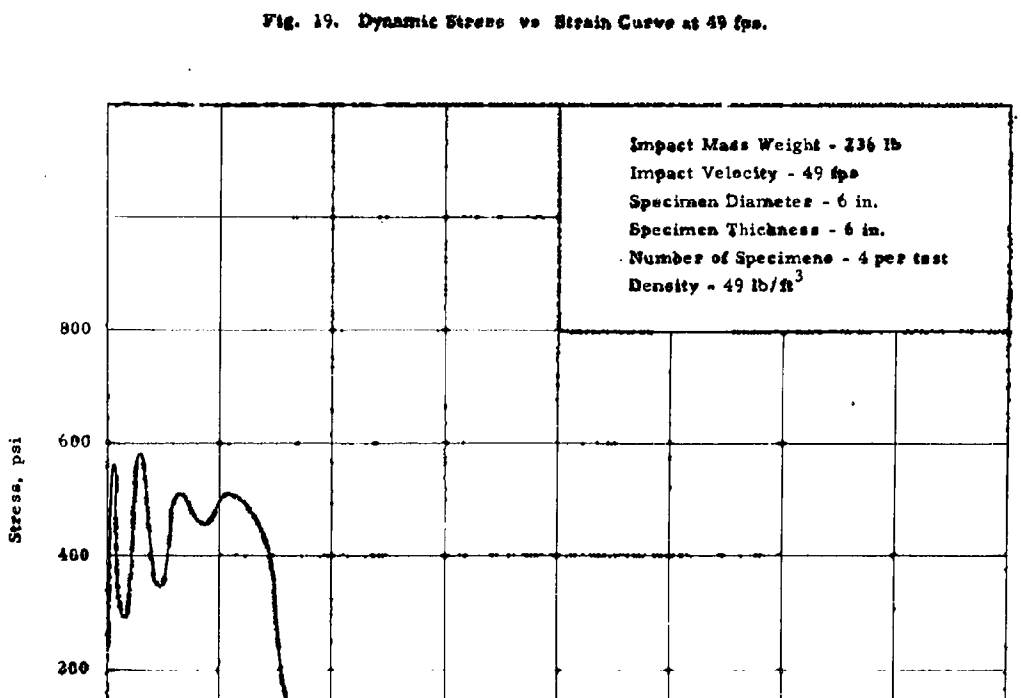

Fig. 20. Dynamic Stress vs Time Curve at 49 fps.

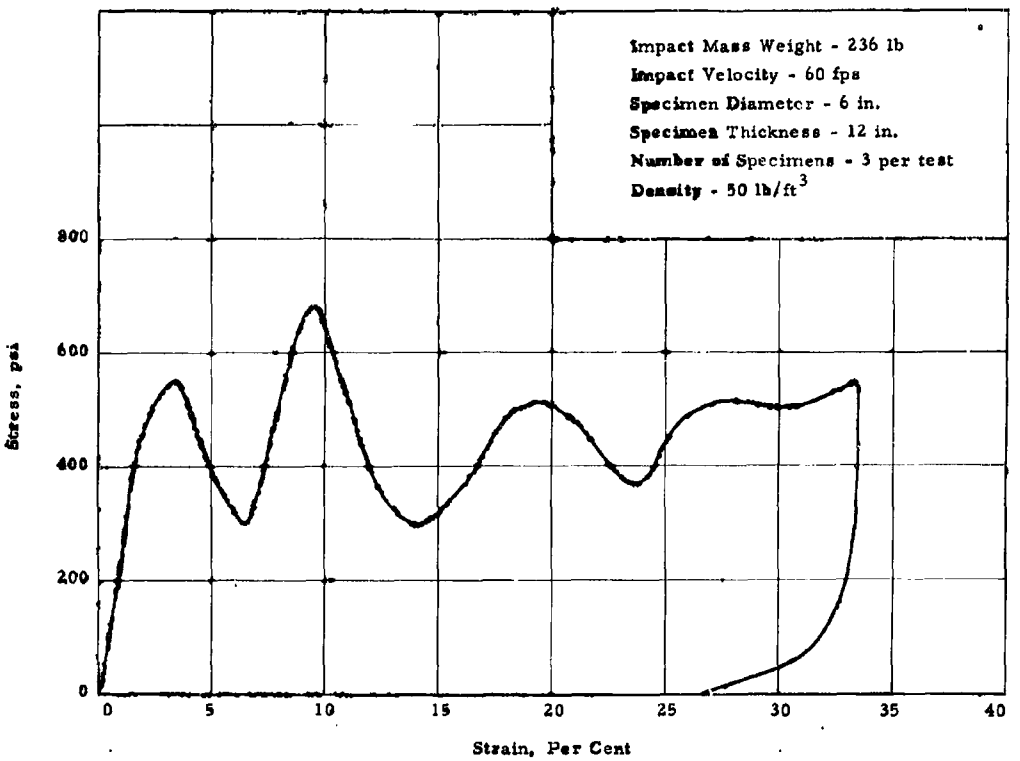

Fig. 21. Dynamic Stress vs Strain Curve at 60 fps.

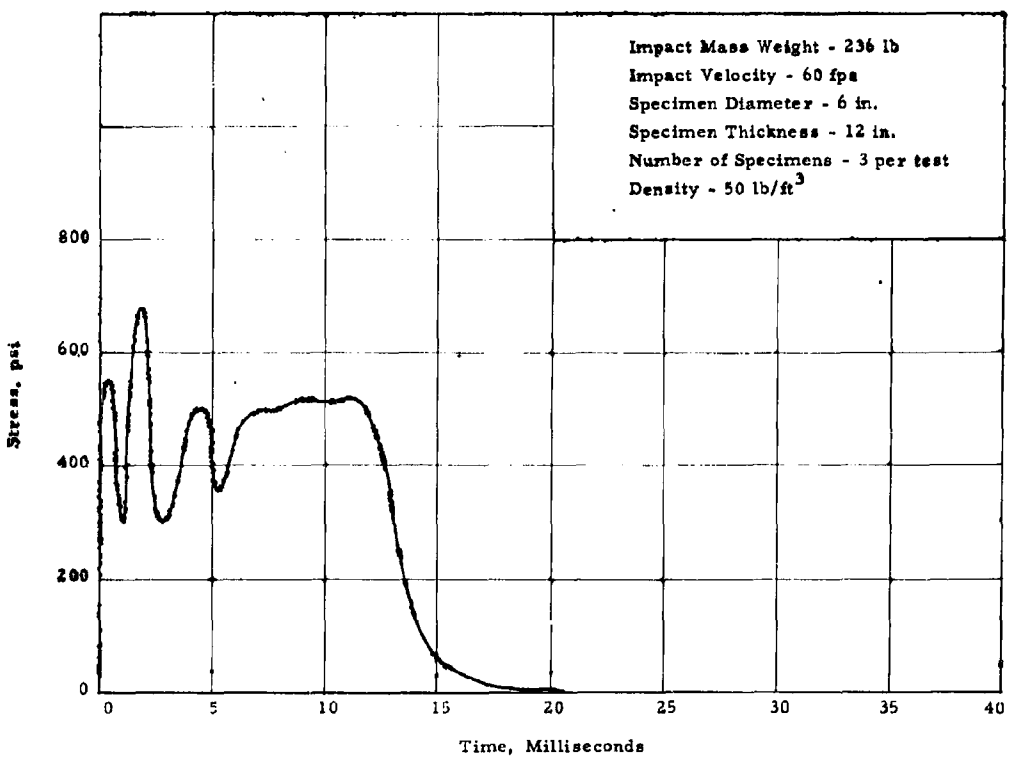

Fig. 22. Dynamic Stress vs Time Curve at 60 fps.

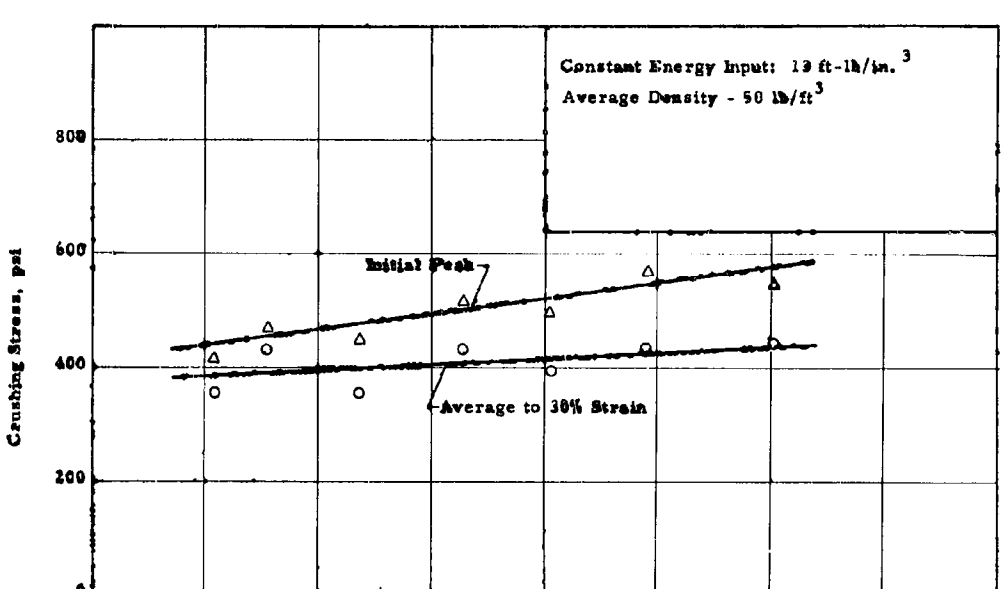

Fig. 23. Effect of Impact Velocity on Crushing Stress.

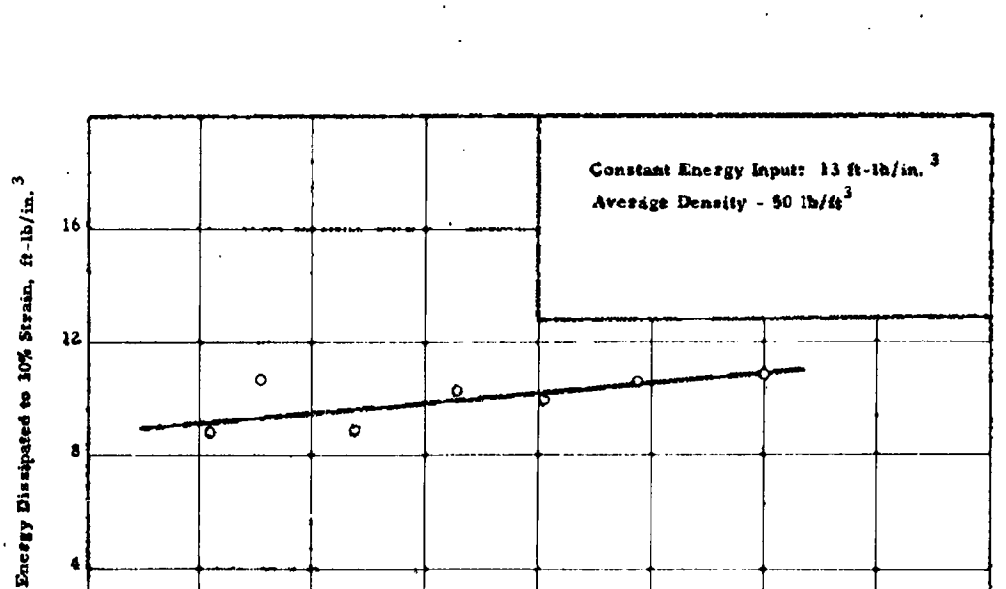

Fig. 24. Effect of Impact Velocity on Energy Dissipated to 30 Per Cent Strain.

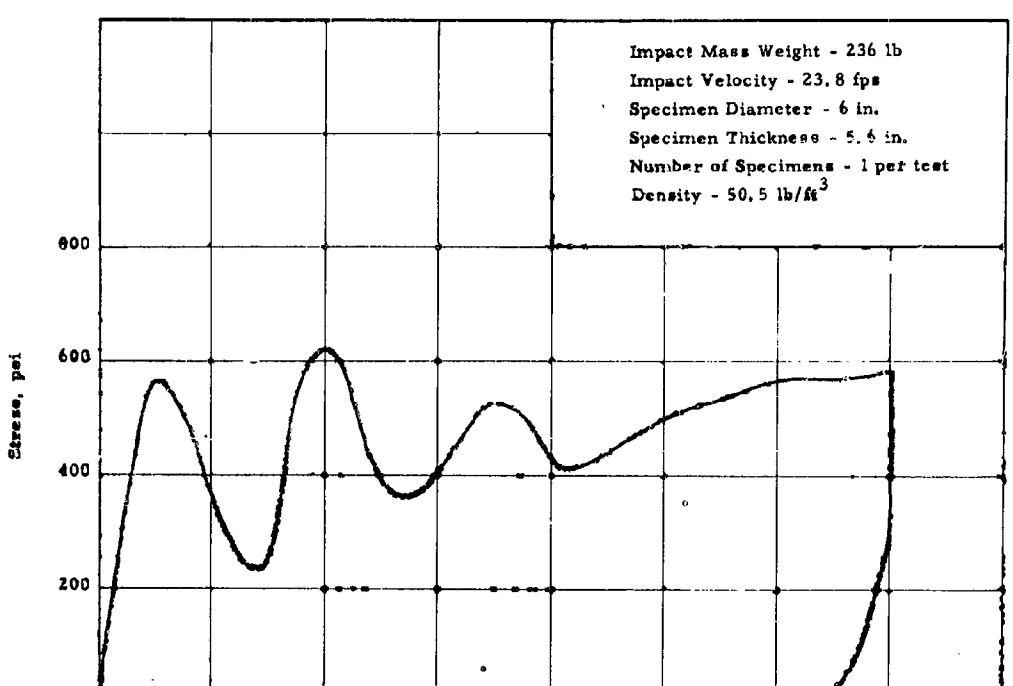

Fig. 25. Dynamic Stress-Strain Curve with 236-lb Impact Mass Weight.

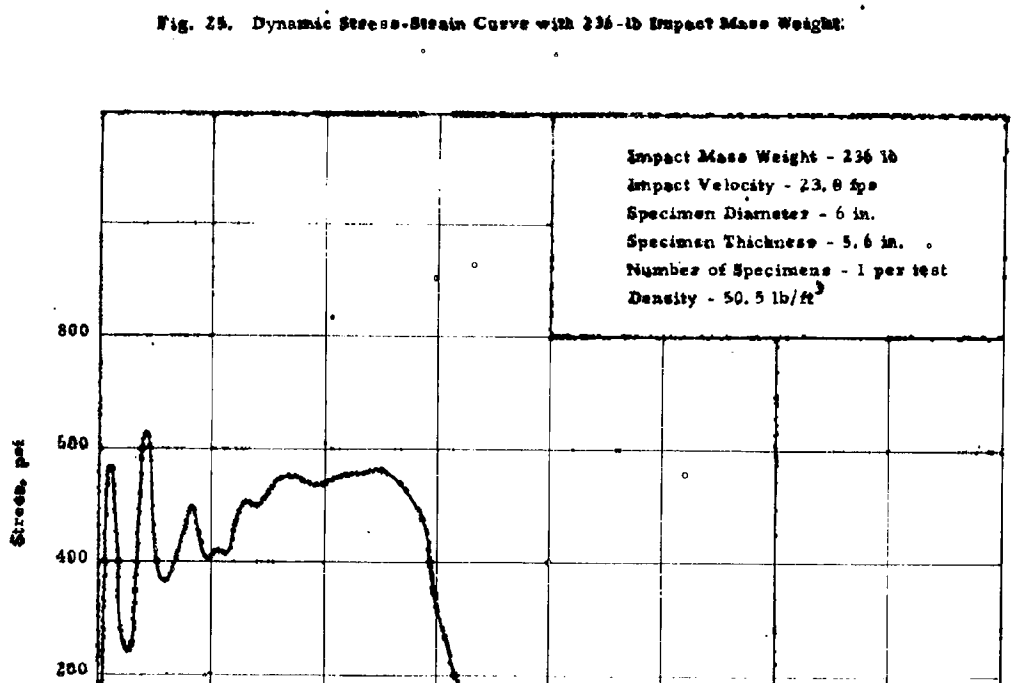

Fig. 26. Dynamic Stress-Time Curve with 236-lb Impact Mass Weight.

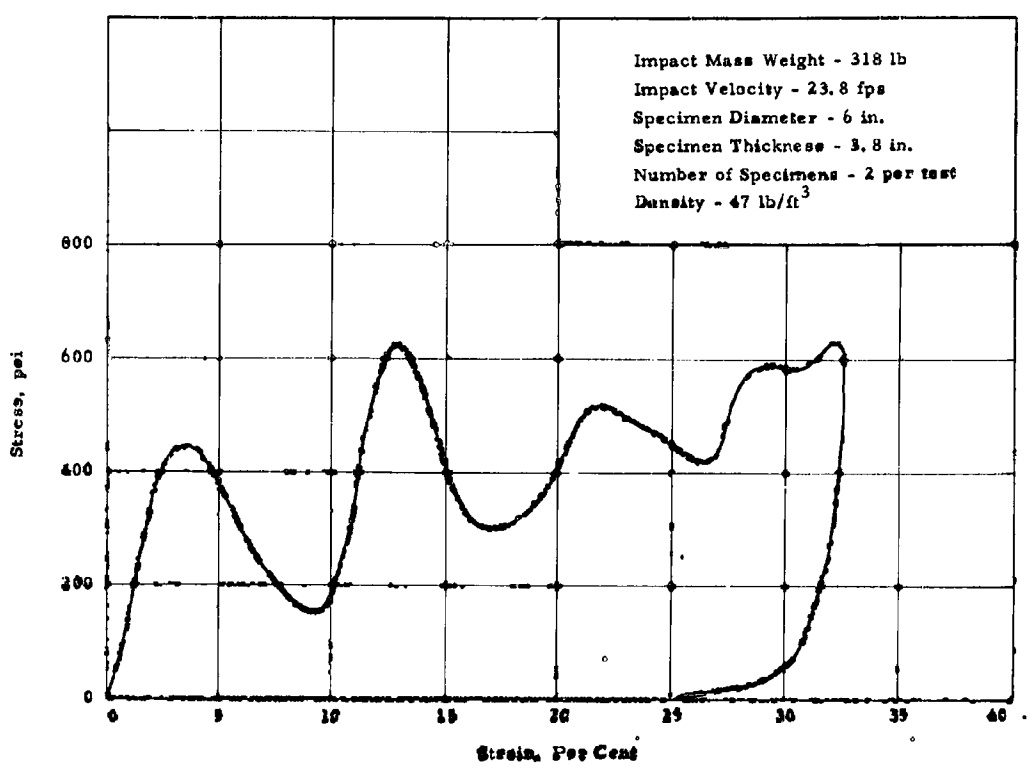

Fig. 27. Dynamic Stress-Strain Curve with 318-lb Impact Mass Weight.

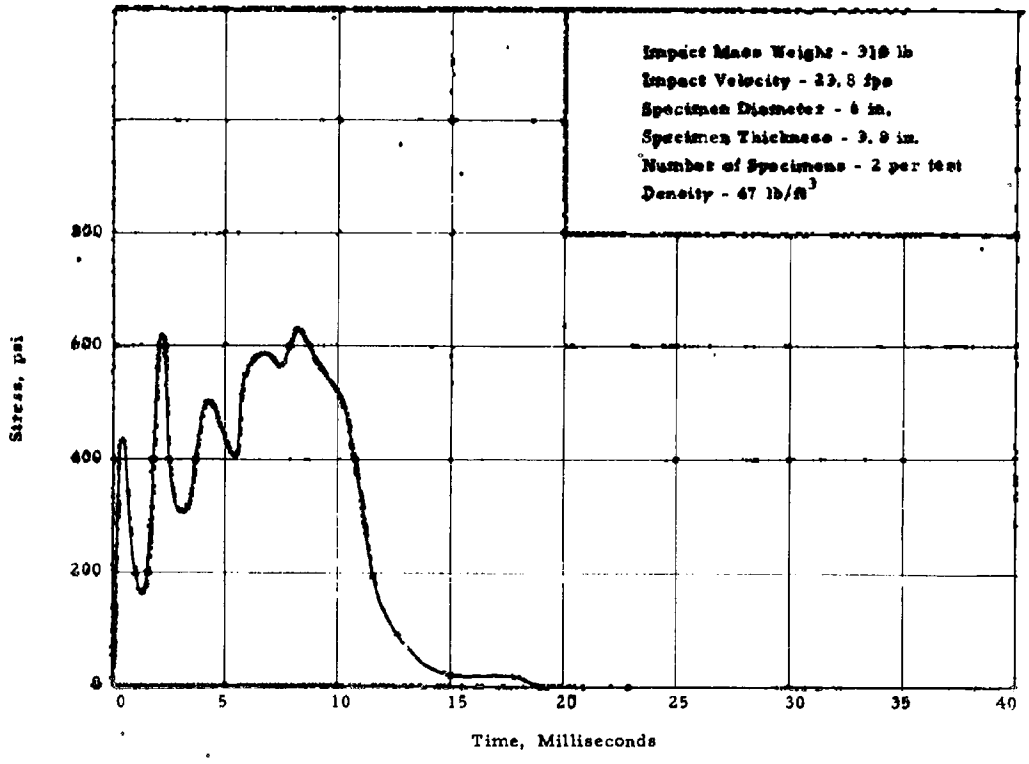

Fig. 28. Dynamic Stress-Time Curve with 318-lb Impact Mass Weight.

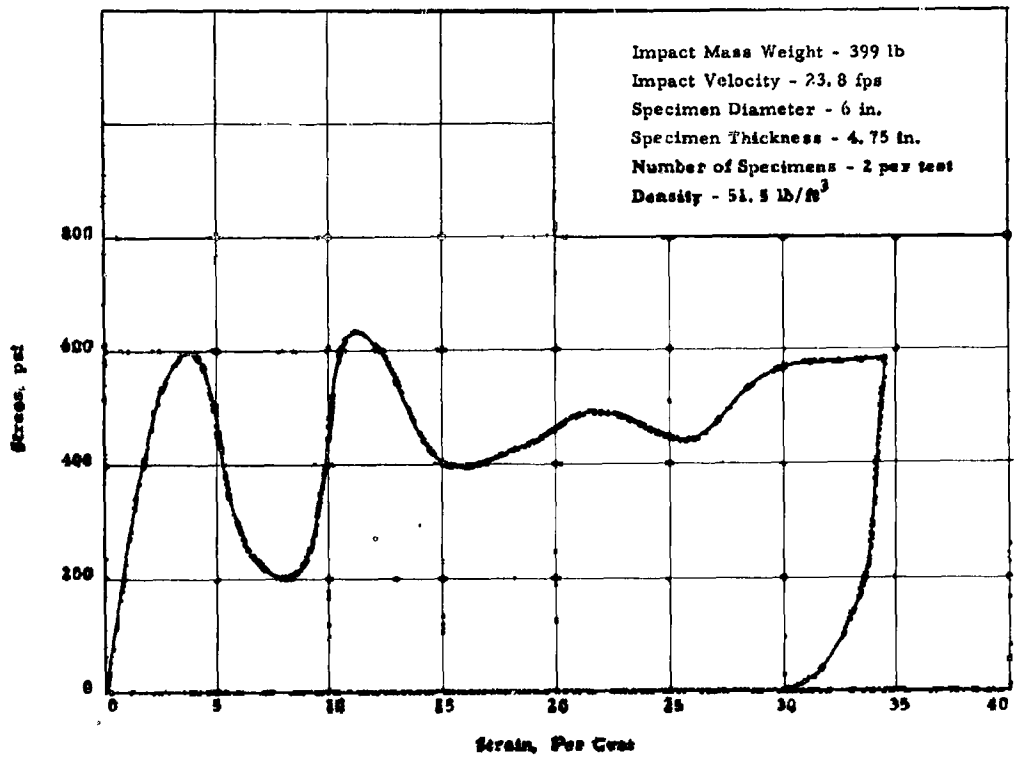

Fig. 29. Dynamic Stress-Strain Curve with 399-lb Impact Mass Weight.

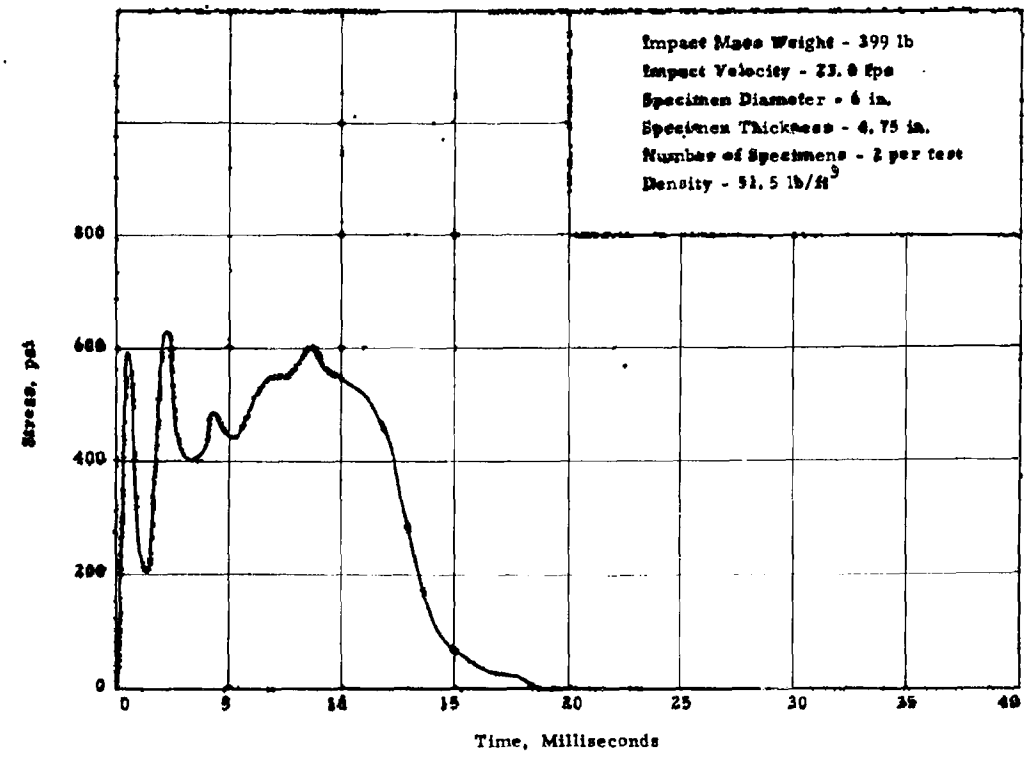

Fig. 30. Dynamic Stress-Time Curve with 399-lb Impact Mass Weight.

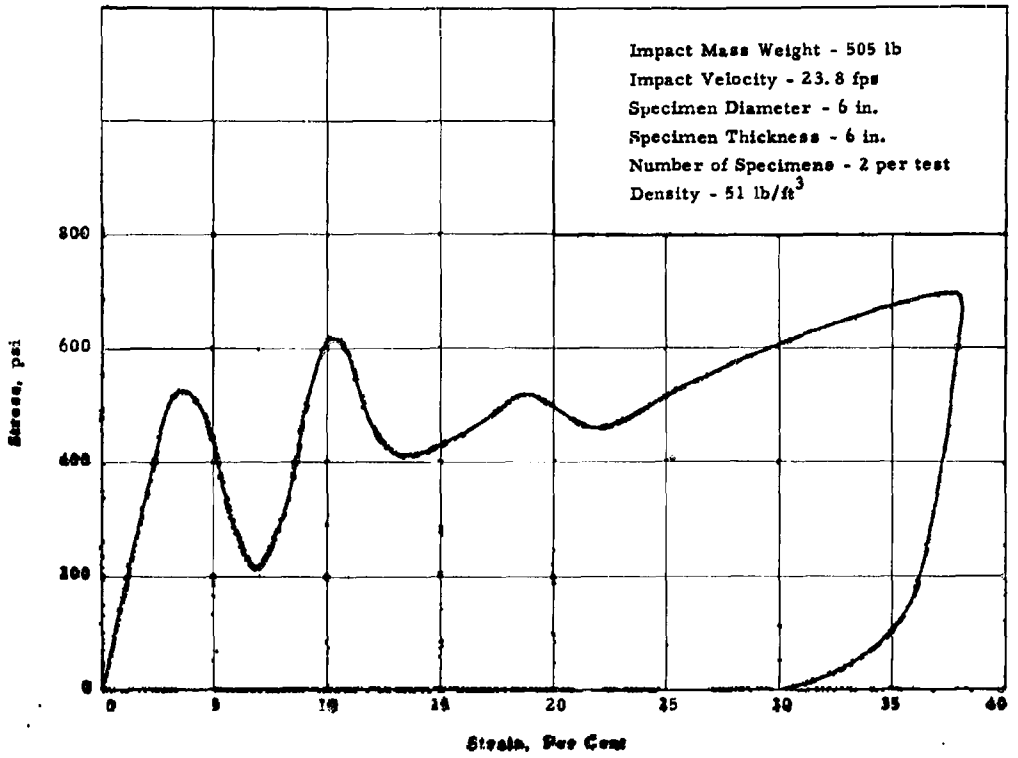

Fig. 31. Dynamic Stress-Strain Curve with 505-lb Impact Mass Weight.

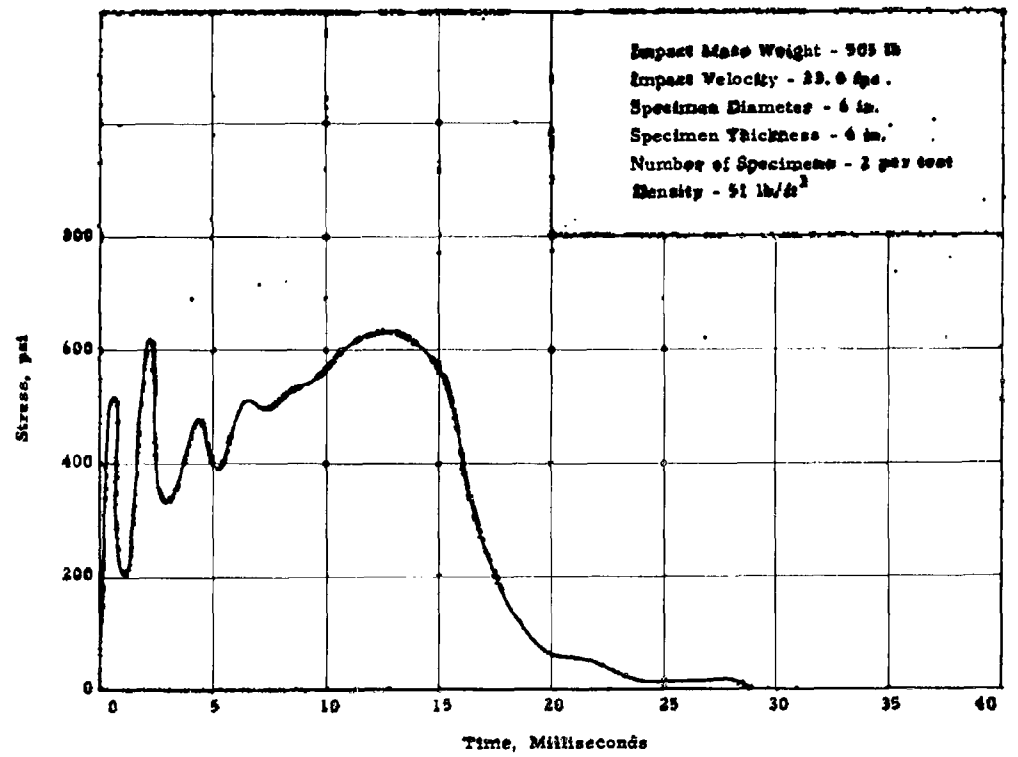

Fig. 32. Dynamic Stress-Time Curve with 505-lb Impact Mass Weight.

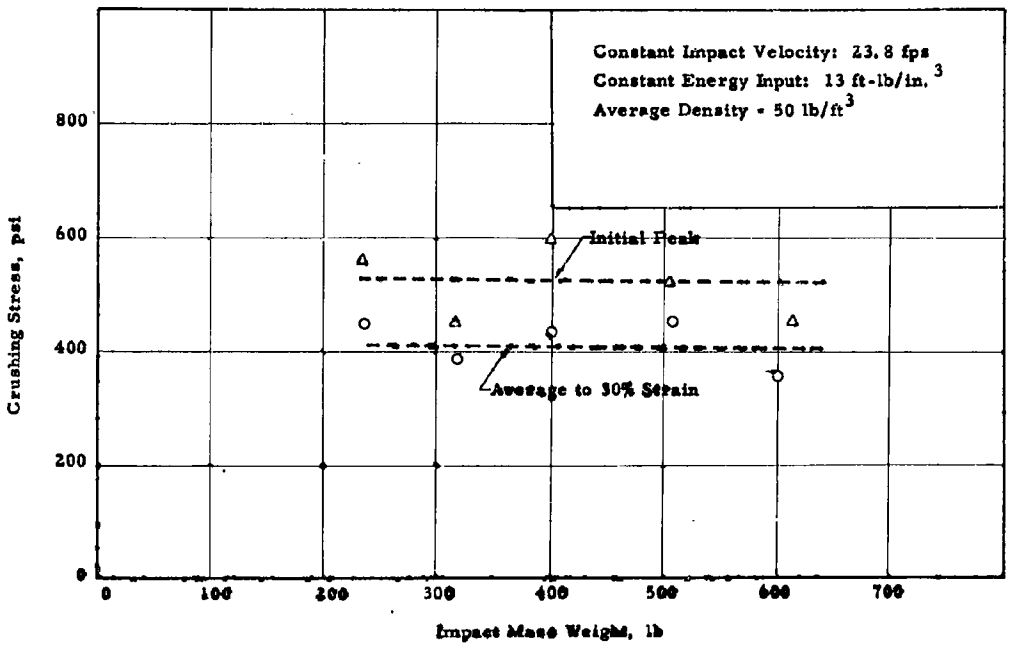

Fig. 33. Effect of Impact Mass Weight on Crushing Stress.

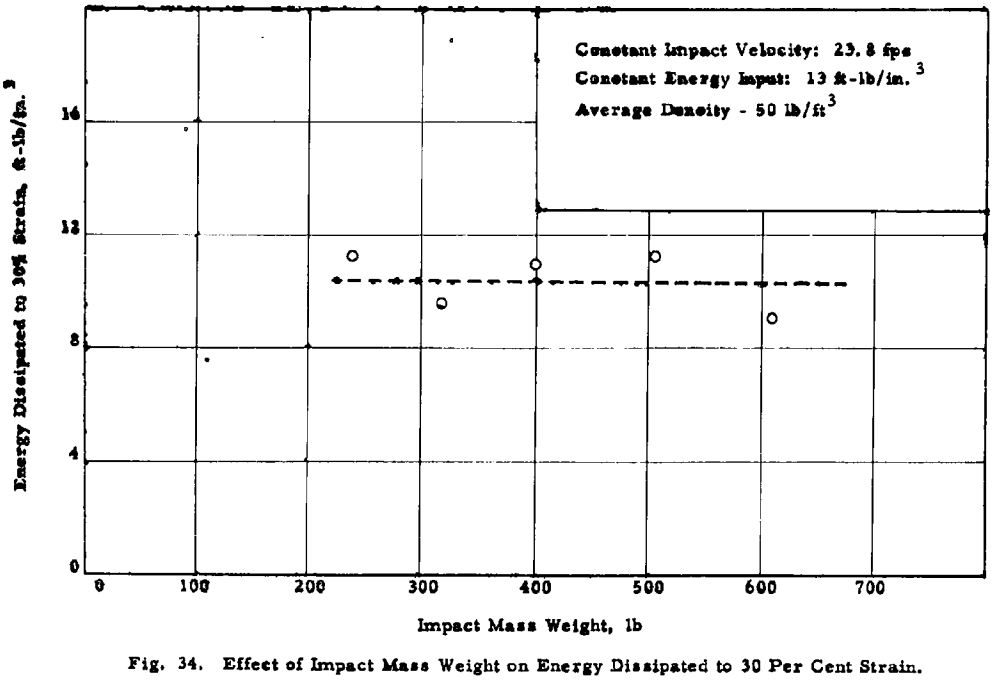

Fig. 34. Effect of Impact Mass Weight on Energy Dissipated to 30 Per Cent Strain.

CONCLUSIONS

All the conclusions apply to the velocity range, 10.8 to 60 fps, and the impact mass weight range, 236 to 611 lb, investigated in this study.

1. The initial peak crushing stress of this vermiculite concrete is between 420 and 570 psi, and the average crushing stress to 30 per cent strain is between 350 and 450 psi.

2. Bottoming begins to occur at 30 to 35 per cent strain.

3. Initial peak crushing stress, average crushing stress to 30 per cent strain, and energy absorbed to 30 per cent strain increase with an increase in impact velocity.

4. Initial peak stress, average stress to 30 per cent strain, and energy absorbed to 30 per cent strain are independent of impact mass weight.

5. The aggregate itself probably absorbs very little energy. Cement paste with a large amount of entrapped air probably would be just as effective as an energy absorber as lightweight vermiculite concrete.

RECOMMENDATIONS

1. The effect of material density on the stress-strain and stress-time curves should be studied.
2. Vermiculite concretes with cement to aggregate volume ratios greater than one to eight should be studied.
3. Foamed concretes with over 20 per cent air entraining should be studied.
4. Variations in concrete moisture content at the time of test should be studied.
5. A further study of the significance of the initial peaks in dynamic curves should be made.

APPENDIX

TABLE I

Test No.	Mass Weight lb	Impact Velocity fps	Specimens Per Test	Thickness in.	Density lb/ft^3	Initial Peak Crushing Stress psi
1	611	10.8	1	3.0	53	440
2	611	10.8	1	3.0	53	405
3	611	10.8	1	3.0	53	410
4	611	15.3	1	6.0	53	480
5	611	15.3	1	6.0	53	510
6	611	15.3	1	6.0	53	440
7	611	23.8	3	4.8	51	450
8	611	23.8	3	4.8	51	465
9	611	23.8	3	4.8	51	440
10	505	23.8	2	6.0	51	490
11	505	23.8	2	6.0	51	510
12	505	23.8	2	6.0	51	600
13	399	32.7	3	6.0	51	580
14	399	32.7	3	6.0	47	470
15	399	32.7	3	6.0	47	480
16	399	23.8	2	4.75	51.5	540
17	399	23.8	2	4.75	51,5	640
18	399	23.8	2	4.75	51.5	600
19	318	40.2	4	6.0	47.5	500
20	318	40.2	4	6.0	47.5	470
21	318	40.2	4	6.0	49	540
22	318	23.8	2	3.8	47	450
23	318	23.8	2	3.8	47	440
24	318	23.8	2	3.8	47	460
25	236	23.8	1	5.6	51.5	600
26	236	23.8	1	5.6	49.5	530

TABLE I
(Cont'd)

Test No.	Mass Weight lb	Impact Velocity fps	Specimens Per Test	Thickness in.	Density lb/ft^3	Initial Peak Crushing Stress psi
27	236	23.8	1	5.6	49.5	560
28	236	49	4	6.0	47.5	550
29	236	49	4	6.0	50	600
30	236	49	4	6.0	50	560
31	236	60	3	12.0	50	600
32	236	60	3	12.0	50	480
33	236	60	3	12.0	50	560

Two static tests were made to determine the curve in Fig. 6. In each test, a laterally confined, 6-in.-dia., 6-in.-thick specimen with a density of 51 lb/ft^3 was compressed.

BIBLIOGRAPHY

1. Karnes, Charles H., James W. Turnbow, E. A. Ripperger, and J. Neils Thompson, High-Velocity Impact Cushioning, Part V, Energy-Absorption Characteristics of Paper Honeycomb, Austin, Structural Mechanics Research Laboratory, The University of Texas, 1959.

2. Turnbow, James W., Cushioning for Air Drop, Part VII, Characteristics of Foamed Plastics Under Dynamic Loading, Austin, Structural Mechanics Research Laboratory, The University of Texas, 1957.

3. Shield, Richard, and Clarke Covington, High-Velocity Impact Cushioning, Part VI, 108C and 100C Foamed Plastics, Austin, Structural Mechanics Research Laboratory, The University of Texas, 1960.

4. Ali, Ahmin, and Hudson Matlock, Cushioning for Air Drop, Part VI, Preliminary Investigation of the Absorption of Shock Energy by Wood in Lateral Compression, Austin, Structural Mechanics Research Laboratory, The University of Texas, 1957.

5. Morgan, Carl W., and Walter L. Moore, Cushioning for Air Drop, Part V, Theoretical and Experimental Investigations of Fluid-Filled Metal Cylinders for Use as Energy Absorbers on Impact, Austin, Structural Mechanics Research Laboratory, The University of Texas, 1956.

6. Ali, Ahmin, Cushioning for Air Drop, Part VIII, Dynamic Stress-Strain Characteristics of Various Materials, Austin, Structural Mechanics Research Laboratory, The University of Texas, 1957.

7. Christiansen, W. J., Relative Vulnerability of Underground Protective Construction, Washington, D. C., Atomic Defense Engineering, Technical Study No. 28, Bureau of Yards and Docks, Department of the Navy, 1959.

8. Vaile, R. B., Jr., Isolation of Structures from Ground Shock, Operation Plumbbob, WT-1424, Menlo Park, California, Stanford Research Institute, 1957.

9. Shield, Richard, Shock-Mitigation with Lightweight Vermiculite Concrete, Austin, Structural Mechanics Research Laboratory, The University of Texas, to be published in 1961.

10. Tapley, Byron Dean, The Effects of Shock-Induced Vibrations on Force-Sensing Apparatus, Thesis, Austin, The University of Texas, 1958.

DISTRIBUTION LIST

Chief of Engineers
Department of the Army
Washington 25, D. C.
Attn: ENGRD-S

Officer-in-Charge
U. S. Naval Civil Engineering Laboratory
Port Hueneme, California
Attn: Mr. Sterling Bugg

Colonel Huie
Air Force Special Weapons Center
Kirtland Air Force Base
Albuquerque, New Mexico

Dr. Harold Brode
Rand Corporation
1700 Main Street
Santa Monica, California

Dr. Robert V. Whitman
Massachusetts Institute of Technology
Cambridge 39, Massachusetts

Mr. R. D. Cavanaugh
Barry Controls, Inc.
700 Pleasant Street
Watertown 72, Massachusetts

Mr. W. R. Perret, 5112
Sandia Corporation
Sandia Base
Albuquerque, New Mexico

Mr. Fred Sauer
Physics Department
Stanford Research Institute
Menlo Park, California

DISTRIBUTION LIST

(Cont'd)

Mr. Kenneth Kaplan
Broadview Research Corporation
1811 Trousdale Drive
Burlingame, California

Mr. William J. Taylor
Terminal Ballistics Laboratory
Aberdeen Proving Ground
Aberdeen Proving Ground, Maryland

Director
U. S. Army Engineer Waterways Experiment Station
P. O. Box 631
Vicksburg, Mississippi
Attn: Mr. G. L. Arbuthnot, Jr.

Dr. N. M. Newmark
111 Talbot Laboratory
University of Illinois
Urbana, Illinois

Commander W. J. Christensen
Bureau of Yards and Docks
Washington 25, D. C.

Dr. Millard V. Barton
Ramo Wooldridge Corporation
5500 West El Segundo
Los Angeles, California

Holmes and Narver, Inc.
849 South Broadway
Los Angeles 14, California
Attn: Mr. Sherwood B. Smith